Research Signpost
37/661 (2), Fort P.O., Trivandrum-695 023, Kerala, India

Bubble and Particle Dynamics in Acoustic Fields: Modern Trends and Applications, 2005: 37-94
ISBN: 81-7736-284-4 Editor: Alexander A. Doinikov

2 Characterisation Of Measures Of Reference Acoustic Cavitation (COMORAC): An experimental feasibility trial

T.G. Leighton[1], P. R. Birkin[2], M. Hodnett[3], B. Zeqiri[3], J. F. Power[1,2] G. J. Price[4], T. Mason[5], M. Plattes[5], N. Dezhkunov[6] and A.J. Coleman[7]
[1]Institute of Sound and Vibration Research, University of Southampton Highfield, Southampton SO17 1BJ, UK; [2]School of Chemistry, University of Southampton, Highfield, Southampton SO17 1BJ, UK; [3]National Physical Laboratory, Quality of Life Division, Hampton Road, Teddington, TW11 0LW, UK; [4]Department of Chemistry, University of Bath, Claverton Down Bath BA2 7AY, UK; [5]School of Natural and Environmental Sciences University of Coventry, Coventry CV1 SFB, UK; [6]Laboratory of Ultrasound Technologies, Belarus State University of Informatics and Radioelectronics P Brovka St. 6, 220027, Minsk, Belarus; [7]Medical Physics Department St Thomas' Hospital, Guy's and St. Thomas' Health Trust, London SE1 7EH, UK

Abstract

There is a need to provide some standard measure for 'cavitation'. This has featured strongly within the requirements of the UK Department of Trade and Industry's National Measurement System Directorate,

Correspondence/Reprint request: Prof. T.G. Leighton, Institute of Sound and Vibration Research, University of Southampton, Highfield, Southampton SO17 1BJ, UK. E-mail: tgl@soton.ac.uk

a body which funds the national measurement system infrastructure within the United Kingdom. Through the Acoustical Metrology programme at the UK National Physical Laboratory (NPL), the UK's requirements for air-borne and water-borne measurement standards and calibrations are met, and this includes underpinning future measurement needs that will enable emerging technologies to be exploited. For some time, it has been realised that it would be exceedingly valuable to be able to offer measurement standards in the area of acoustic cavitation. These would allow workers to make reliable measurements which are potentially traceable to a national standard. A variety of measurements have potential utility in characterising cavitation, and for several decades, across many nations, there have appeared calls for one technique or another to be adopted. Prior to the study reported here, there had never been a comparative study of how various techniques which can be used to monitor cavitation perform under the conditions which might be expected of a practical 'cavitation measurement system'. Key to such a test would be the provision of some repeatable 'amount' of cavitation. The then National Measurement System Policy Unit (NMSPU) directed the NPL to provide this, as part of a research programme investigating and underpinning the establishment of suitable characterisation techniques in the 1998-2001 Programme. Following collaborative studies between NPL and the University of Southampton on the requirements for the measurement of high power ultrasound and cavitation, and the subsequent establishment at NPL of relevant power ultrasound facilities, in 1999 the COMORAC test was proposed. In this, a range of sensors were brought to the NPL standard cavitation facility and compared, not only in their output when measuring a given field, but also in terms of their ability to complete a measurement in an unfamiliar laboratory within tight time constraints. In all, thirteen systems were tested (plus subsidiary tests, for example, both to map and to quantify luminescences). This chapter describes the results, and a discussion of the strengths and weaknesses of each system, together with an evaluation of their usefulness as a potential cavitation measurement method.

1. Introduction

1.1 Background

High power ultrasound and acoustic cavitation are important across a wide range of application areas, from industrial processing to medicine [1] (figure 1). Whilst significant progress has been made recently to understand the mechanisms responsible for the observed effects, there is still a lack of standardized characterization techniques in this technically demanding area. In 1996 a collaboration of the National Physical Laboratory (NPL) and the Institute of Sound and Vibration Research (ISVR, University of Southampton)

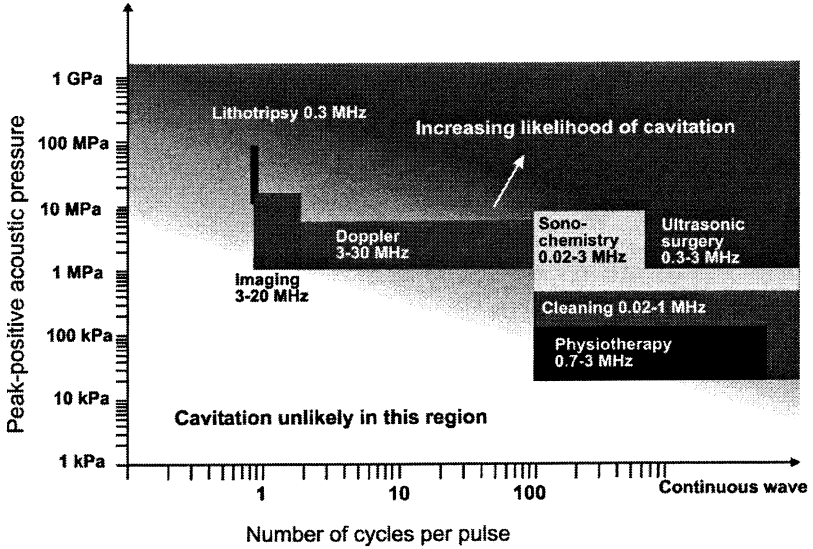

Figure 1. A rough schematic of the acoustic pressures and pulse lengths employed in some of the applications of ultrasound. Parameters are meant as a rough guide only. If an application lies outside the zone where 'cavitation is unlikely' this by no means indicates that cavitation may occur in that application: this would depend on a number of factors, not least the likelihood of nucleation in the liquid sample in question.

was commissioned by the UK Department of Trade and Industry (DTI) to examine the need for standardisation of measurement methods for high power/cavitating ultrasound fields. The results of this project [2,3], which included compiling and analysing the views of almost 70 experts worldwide, demonstrated that there is a significant need for standardisation.

Based on these findings, NPL carried out two further projects in the area of high power ultrasound. The first was to produce an ultrasonic cleaning vessel to be used as a reference cavitation source [4]. The second project was to collate the opinions of international experts as to the feasibility of establishing a reference cavitating medium [5].

A reference for cavitation would comprise a stated medium, sound field, and detector, plus a scale or end-point (based on threshold, activity etc.). The recent projects outlined above [4,5] were aimed at producing the reference sound field and medium. Therefore the first author proposed and put together COMORAC ("Characterisation Of Measures Of Reference Acoustic Cavitation"), a trial to investigate the attributes of a range of sensors, with a view to illuminating the aspects of possible future 'standard sensors' (both primary and

secondary) which should be considered. Whilst clearly there is more general applicability, the emphasis would be on sensors designed to measure cavitation in ultrasonic cleaning baths, which would have the capability of operation in continuous-wave fields containing high time-averaged void fractions [6]. Therefore, whilst at the time of COMORAC there existed sensors designed for cavitation detection in the more sparsely cavitating biomedical fields, including active [7-9] and passive [10-13] acoustic cavitation detectors, the trial was not designed specifically to test these sorts of devices (although in fact the passive detector of Coleman *et al.* [10,11] was judged appropriate for inclusion). The resulting COMORAC experiment is the topic of this report.

The key characteristic of this experiment was that the devices were tested under suboptimal conditions, of the type which they might encounter were the device to be adopted by an industry for use in the workplace. Cavitation detectors tend to be characterized by their inventors in their own laboratories. Whilst this might be appropriate for devices intended to be 'gold standards' for a cavitation reference, a secondary standard or a workable device for industry should produce stable and reliable results when operated in other environments, by other people in a restricted timescale. Whilst two of the sensors used in COMORAC (foil and particle erosion) were introduced on an opportunistic basis without prior testing, the other 11 sensors used in this trial worked well in their home laboratories. However many performed less well during COMORAC, and indeed some have undergone important redesign following COMORAC which have improved them enormously.

1.2 Previous suggestions for standard sensors

Both the published literature and the marketplace contain devices to 'measure cavitation'. However to our knowledge none have been through the level of cross-comparison involved in COMORAC, nor have they been subject to COMORAC's requirement that the test site be unfamiliar and test time be rigidly imposed and constrained. Most commercial devices refer to a scale which bears no clearly stated relation to a physical aspect of cavitation.

According to the survey discussed above [3], the majority of industrial contributors stressed the importance of 'measuring' cavitation in ultrasonic cleaning baths. This is not new: as early as 1964, standard chemical procedures for cleaning baths were proposed [14,15]. Crawford's report [16] includes Weissler's discussions [17] on the use of a colour measure of the sonochemical liberation of chlorine from carbon tetrachloride as a method of characterising ultrasonic cleaning baths. Recognising the role of cavitation in both the operation of such baths and in the sonochemical test he describes, Weissler attempted to formulate the cleaning ability of, say, an ultrasonic bath, in terms of a summation $\sum_i a_i n_i$ over all classes i of cavitation event. He introduced a

weighting a_i appropriate to the cleaning effectiveness of that event, with n_i being the number of events in class i per second per unit volume. Weissler recognised that the n's are functions of temperature, frequency, dissolved gas content, treatment time, location of the test site within the cleaning tank etc., and suggested that a double integral of $\sum_i a_i n_i$ over the time of treatment and the specified volume constitute an improved expression. Weissler introduced a similar expression $\sum_i b_i n_i$ for the sonochemical effect of the cavitation, where b_i is the coefficient of the relative sonochemical effectiveness of each class of cavitation. Weissler proposed measuring the sonochemical activity of the cleaning bath and then, by assuming that the ratio a_i / b_i is constant at least for a particular cleaning bath at a particular frequency, extrapolating to determine the cleaning effectiveness of the bath. Such an approach may be of limited value given the range of possible cavitation effects, not just involving the various activities a single bubble can undertake [18], but also cloud effects (acoustic shielding, local degassing, cluster collapse etc. [19]). In addition, though it should be possible to detect individual events at low levels of cavitation, it would be very difficult to do this during intense cavitation, and it is no simple matter to assign an efficacy to each event.

Following the work of Weissler [17], Crawford [16] proposed the use of aluminium foil as a standard material for measuring cavitation in terms of the degree of erosion. He described how, when immersed in a cavitation field, the foil first dimples (dimples are closely packed and around 0.1 mm diameter). The foil is then punctured as the dimples form 'pinholes'. With erosion commencing from the ragged edges, the pinholes then expand and may coalesce. In a cleaning bath this stage can be reached in 15-20 s for a foil thickness of ~10 μm. Sections of the foil detach as the coalescence continues. In a 500 W cleaning bath, operating at 20 kHz, Crawford recorded the 'destroyed area' (measured using light transmission) as a function of the exposure time. He observed that generally up to 35% of the area of the foil was destroyed before coalescence caused larger pieces of foil to detach. He proposed an index found by obtaining the product of the proportion of the area eroded and a constant reflecting the thickness and type of the foil, and dividing this product by the time of sonication. Crawford considered it to be a first-order solution to allow, for example, a comparison between baths, or a day-to-day check on the operation of an individual bath.

Boucher and Kreuter [20,21] also examined techniques for the measurement of the efficacy of cleaning baths. Although they discussed sonochemical [17,22] and erosive methods, the technique they favoured is based on the integration of cavitation noise [23] after elimination from the data of the transducer signal [24]. They propose a unit of cavitation, the CAVIT

[20,21], quoted as follows: "The CAVIT is the one hundred seventy fifth of the amount of cavitational energy released in a tank (5½" wide by 9⅜ " long by 4" deep) filled with 2½ litres of partially degassed water when irradiating 18 W of acoustic energy [*sic*] in the liquid at a frequency comprised between 35 and 37 kcps and within a temperature range of 26° and 27°C. Under the above stated conditions a pure lead sheet (4" wide by 8" long by 1/16" high) placed in horizontal position inside one of the maximum erosion zones will lose 0.44% of its initial weight after one hour of insonation starting at a temperature of 26°C. Also under the above stated condition 2½ litres of the Weissler reagent poured directly into the tank will give a light transmittance of 50% after 1190 seconds of irradiation".

The same range of techniques was discussed in a 1963 report of the American Standards Association [25] with respect to standardisation of cleaning baths. While recognising the importance of spatial resolution, it recommended quantitative soil removal rate as a primary standard, with chemical or physical phenomena being selected as secondary standards "for reasons of simplicity or cost", provided that the activity measured for the secondary standard should bear a consistent quantitative relationship with the primary. Two tests are discussed from each category: the removal of soils containing a radioactive isotope, and of dyed grease (which, after sonication, is removed from the test piece by solvent, which in turn becomes coloured to a degree dependent on the amount of soil remaining); chemical reactions, including chlorine release [16]; and the physical effects of lead erosion (rejected as a primary standard because of poor reproducibility at the time) and foil rupture (discussed in the context of a qualitative, rather than quantitative, indicator). Finally, cavitation noise was investigated. The preferred measure in the report was soil removal, partly because it is a direct measure of the quantity of interest to users of cleaning baths. In the event that a good soil cannot be found, the authors recommend that a chemical test be the primary standard. One suggested trial solution for a standard soil, the removal of which would provide a measure of the 'cavitation' that has occurred, was graphite pencil lines on ground glass; however this has proved to be extremely difficult to standardise [16].

In 1963, an American Standards Association report [25] distinguishes between different types of cavitation activity. 'Type A' measures of cavitation activity are those based on physical effects such as radiated sound, whose value at a point in the liquid depends on events scattered throughout the cavitation field. 'Type B' measures are based on physical effects (e.g. a chemical reaction) that are localised at or near to the cavitation event which give rise to the effect. The report [25] suggested that if only statistical averages can be measured, then Type B measures of cavitation activity might indicate

the 'average violence of cavitation events occurring within a small volume in a specified time interval'.

1.3 Specifications for COMORAC

It is important to appreciate that any reference system for cavitation must comprise three components: the reference sound field (which necessarily includes a reference vessel in which the liquid is contained); a reference liquid; and a reference detection system to monitor the effects of cavitation. In the words of Apfel (1984): "*Know thy liquid; know thy sound field; know when something happens.*"

The manifestations of these three factors in the COMORAC test are not meant to be a complete solution, but rather reflect those conditions which could be set up within the scale of the test, and which proffer an adequate test base. The vessel and liquid components had been chosen by NPL and established prior to COMORAC as a result of their studies [4,5]. The purpose of COMORAC was to set up a test protocol which would identify the requirements that would be placed on a sensor which would either be incorporated as the third component in the reference; or, once calibrated against the reference, could be used to 'measure cavitation in the field.'

In practice, in order to assess the viability of any one of these three components, it is necessary to have already found satisfactory solutions for the other two components (figure 2(*a*)). This 'Catch-22' situation cannot be resolved in a single COMORAC experiment, but rather be iteratively solved by staging a series of COMORAC tests. Each test will identify how the three components (sound field, medium and sensor) can be improved prior to the next COMORAC test.

It should be noted that this first COMORAC experiment was completed relatively early within the standards development programme at NPL. In order to make rapid progress in developing a reference system and to gather expertise in the technical field, it was deemed essential to purchase an 'off-the-shelf' item in terms of the vessel itself, rather than have a bespoke system designed and manufactured. Consequently, care needs to be exercised in using the term 'reference' when applied to the cleaning vessel forming the test bed for these measurements. The 'reference' used for this purpose is likely to be, in fact almost certainly will be, non-ideal in terms of a number of features of its performance, such as the non-uniform spatial distribution of acoustic pressure and cavitation activity, as well as, possibly, temporal stability. Nevertheless, it was considered appropriate for use as a basis for the COMORAC tests.

It should be noted that the words of Apfel, quoted above, specify the *minimum* criteria that must be met if a reference for cavitation is to be produced. This is because they refer to the *threshold* for cavitation, and not to

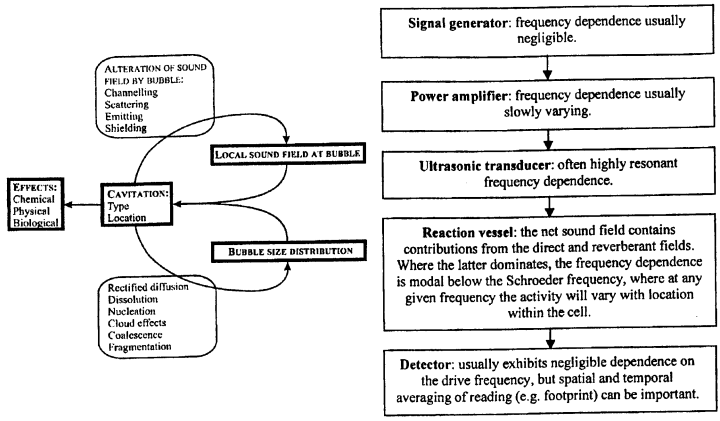

Figure 2. (*a*) The chemical, physical and biological effects of cavitation depend on both the type of cavitation (e.g. inertial, noninertial, jetting, fragmentary) and its location. Both of these factors depend strongly on the local sound field at the bubble and on the sizes of bubble present in the population. These two together, for example, characterise the inertial cavitation threshold, and also the locations to where bubbles might migrate and accumulate under radiation forces (depending on the other relevant forces present, e.g. flow, turbulence, streaming *etc.*). Such accumulations will in turn affect the local sound field, through the processes of channelling, dispersion, absorption, diffraction, scattering and shielding, and will affect the bubble size distribution through their influence on the processes of coalescence, fragmentation, rectified diffusion and shape stability. As a result, the observed effect depends on the characteristics of the cavitation, which are determined by the local sound field and the bubble size distribution. However there is feedback from the cavitation, which influences these two key parameters. Reproduced from Leighton [19]. (*b*) Diagram showing the components and their various frequency dependencies commonly employed in sonochemical experiments (after Birkin *et al.* [26]).

the degree of cavitational 'activity'. The latter is quantified through measurement of some effect produced by cavitation, be it luminescent, chemical, acoustic, erosive, biological etc. Hence to measure cavitational 'activity', it is necessary to understand what is being measured, and its place amongst the other effects. It is for example no use basing a sensor to monitor the efficacy of cleaning baths on acoustic emission if that emission bears no relation to the amount of cleaning which occurs. Birkin *et al.* [26] attempted to identify the existence, or otherwise, of such correlations. A cylindrical sonochemical reactor was driven at frequencies from 20-160 kHz, with frequency increments as small as 1 kHz. Over the same frequency band, a

hydrophone was used to monitor the acoustic pressure at three locations within the cell. A number of experimental parameters which reflect cavitation were monitored: multibubble sonoluminescence (MBSL), multibubble sonochemiluminescence, degradation of an organic species (medola blue), the Fricke reaction, the Weissler reaction, hydrogen radical trapping using the formation of $CuCl_2^-$, and the emission of in-air broadband acoustic signals across the audio frequency range as the drive frequency varied from 20-160 kHz. Strong correlations were observed between both luminescences and the sonochemical reaction rates. The peaks in activity followed the frequencies at which strong modal structures occurred within the reactor [6, 26], rather than reflecting the resonances of the drive transducer. The in-air acoustic emission did not correlate so well with the luminescences and sonochemical indicators. Measurements of the drive acoustic pressure amplitude, which was measured at only three locations in the cell, could be used to predict at which frequencies cavitation (and hence sonochemical activity) would be initiated: when a peak in one occurred, a peak in the other was seen. However the relative magnitudes of the peaks in drive pressure amplitudes did not reflect the relative magnitudes of the peaks in sonochemical activity. These results were interpreted in terms of the frequency dependencies of the various components of the system (figure 2(*b*)).

In summary, the reference ultrasonic vessel and liquid having been ordained prior to the test, the purpose of COMORAC was to assess what might be the requirements looked for in any sensor proposed to function as the third component of this reference system. Because of the 'Catch-22' situation described above, it was realised that a single COMORAC experiment would be unlikely to produce a final reference system. However this experiment would test protocols, and the results would identify refinements to the vessel, medium and sensors which it would be desirable to undertake before the next COMORAC test.

1.4 Schedule for COMORAC

The coordinator (TGL) invited the participants to submit a proposed device and measurement scale. They were then invited to visit the NPL at a set time and place and, against their stated scale, produce a measure of the cavitational activity which was generated in NPL's prototype reference ultrasonic cleaning bath. Funds were provided for travel only, and not for sensor development. COMORAC was to cover four pairs of consecutive days at NPL, although in fact the final sensor (focused bowl) was only available for one day because of national petrol strikes (see Table 1). Each researcher was allotted one pair of days in which to deploy the range of sensors they brought to the experiment (which ranged from 1 to 4, depending on the researcher). The exceptions to this were the NPL and University of Southampton (UoS)

Table 1. Schedule of the tests in COMORAC. The Stage Three tests coincided with national petrol shortages, which prevented TGL, PRB, TM and AC from attending. For each date the tests are listed in the chronological order in which they were tested.

STAGE ONE COMORAC TESTS

Thursday 17 August 2000 and Friday 18 August 2000
Personnel: Tim Leighton (TGL), Peter Birkin (PRB) and John Power (JFP) (University of Southampton, UoS) visit Mark Hodnett (MH) and Bajram Zeqiri (BZ) at NPL.
Devices tested: Sonochemiluminescence, sonoluminescence, high frequency acoustic emission (PCS), foil erosion.
Vessels used: NPL reference cleaning bath. Note the PCS sensor was used extensively throughout the tests. As such this device received the most erosive abuse of all the systems employed.

STAGE TWO COMORAC TESTS

Tuesday 29 August 2000
Personnel: Gareth Price (GP) (University of Bath) visits PRB, JFP and TGL at UoS.
Devices tested: Terephthalic acid, Fricke reaction.
Vessels used: A cylindrical cell [6] was set up at UoS in order as a practice ground prior to visiting NPL.

Wednesday 30 August 2000 and Thursday 31 August 2000
Personnel: TGL, PRB, JFP (UoS), and GP (University of Bath) visit MH at NPL.
Devices tested: Chemiluminescence, sonoluminescence, Fricke reaction, terephthalic acid, high frequency acoustic emission (PCS), Weissler reaction, electrochemical erosion.
Vessels used: NPL reference cleaning bath

STAGE THREE TESTS

Monday 11 September 2000
Personnel: Mario Plattes (MP) (University of Coventry) visit MH and BZ at NPL.
Devices tested: Calorimetry, high frequency acoustic emission (PCS).
Vessels used: NPL reference cleaning bath

and

Personnel: Nikolai Dezhkunov (ND) (Belarus State University, BSU) visits PRB, JFP and TGL at UoS.
Devices tested: Subharmonic emission (IC-3).
Vessels used: Southampton cylindrical cell.

Tuesday 12 September 2000
Personnel: JFP (UoS) and ND (BSU) and MP (University of Coventry) visit MH and BZ at NPL.
Devices tested: Calorimetry, high frequency acoustic emission (PCS), subharmonic emission (IC-3).
Vessels used: NPL reference cleaning bath

Wednesday 27 September
Personnel: Andy Coleman (AC) (St. Thomas' Hospital) and TGL PRB, JFP (UoS) visit MH and BZ at NPL
Devices tested: High frequency acoustic emission (focused bowl hydrophone), Weissler reaction.
Vessels used: NPL reference cleaning bath

researchers, who attended more often so that the former could operate and monitor the reference cleaning bath, and so that the latter could facilitate coordination and simultaneous deployments. In addition some researchers took up the option of first trying out their sensors on a 'practice ground', a cylindrical cell cavitation vessel set up at the UoS [6].

In comparing the results between sensors, the *a priori* assumption had to be made that, for a given 'drive' setting for the NPL reference bath (stated as a volumetric power density – see section 2.1), a 'steady amount of cavitation' was produced. Of course, without a satisfactory detector this could not be proved unequivocally, and such a detector would at the very least require the completion of the COMORAC study. However within their ability to monitor it, NPL were satisfied with the stability of their system over a limited range of temperatures and water types. Measurements carried out over an extensive period of 18 months had, prior to COMORAC, shown that the cavitation activity in the bath (defined by the broadband energy contained in the spectrum measured by a Bruel and Kjaer hydrophone) was reproducible to ±12 % [4].

The problems with, and need for, a study such as COMORAC are illustrated by the fact that in writing about cavitation, one would like to use phrases like 'a steady amount of cavitation' but its meaning is far from clear. Hence the following requirement was placed upon those who were invited to participate in COMORAC (the authors of this paper). This was, specifically, that prior to the start of the test they had to provide the coordinator with detailed specifications of the operational parameters of their device: detector footprint; the temporal and spatial resolution and averaging; limitations with respect to linearity and saturation; noise floor; spatial and temporal resolution and averaging; whether it responds to the threshold for cavitation, or the amount of an effect (erosion, acoustic emission, sonochemical effect etc.) which is a product of cavitation. It was also necessary to ascertain to what degree the authors understood what phenomena (both cavitational and non-cavitational) can give a measurement signal: a subharmonic signal, for example, can be generated by both inertial and non-inertial cavitation. Indeed, given that many of the sensors interpreted an electrical current in terms of a stated cavitational indicator (e.g. cavitation noise), then it is important to understand what non-cavitational components in the complex environment of a cleaning bath (e.g. pyroelectric effects, electrical interference, erosion etc.) could contribute to the current.

The requirement that the authors make their measurement, not in their own laboratory but at NPL, and on a specified date, imposed performance and reliability constraints which must be expected of a commercial cavitation sensor. The results can only be interpreted as a feasibility study, the first in the series of COMORAC experiments that would be required to iterate to a reference solution. For example, insufficient time was available to optimise measurements or make repeat visits to retake data, to investigate their repeatability and reproducibility, or to check the long-term stability of the device. Nevertheless this study serves two purposes: it casts light on what questions must be asked of proposed sensors; and it indicates the very minimum testing a putative commercial or research 'cavitation measuring

device' should be subjected to before publishing the manner of claims which are all too common in research literature and advertising.

In summary therefore, the coordinator invited the participants to submit candidate sensors and measurement scales; and provide detailed specifications as listed above. Once these had been finalised, the authors were allocated a 2-day period in which they were able to use their sensors to monitor the output of the NPL reference system as it was driven at various volumetric power densities (see section 2.1). The final requirement was that the results, which could be obtained through post-processing if required, were supplied to the coordinator for further processing and correlation. These results had to be accompanied by an account of the random uncertainties in the form of error bars that represented the standard error in the mean for a stated number of measurements.

2. Experimental method

2.1 Reference facilities at NPL

The reference ultrasonic cleaning bath at NPL is described in detail elsewhere (see [4, 5]). The rig is shown in figure 3. The cleaning bath used in this system was a Branson bath, operating at 40 kHz, with 12 transducers. It had 1 kW nominal power (90% efficient), internal dimensions 500 x 300 x 400 mm. The internal surface of the wall was stainless steel. The power output was adjustable at a coarse level locally, or with finer resolution via a power supply. It is the nominal power densities supplied by the manufacturers which are plotted on the abscissa in the results (section 3) as volumetric power density against which all the data are plotted. These are calculated assuming that, at 100 % excitation, 900 W of acoustic energy is dispersed into 18 dm^{-3} of liquid. It should be noted that these estimates of the volumetric power density are significantly greater than those estimated by calorimetry (section 3.5). Unless otherwise stated, the graphical results presented in this paper were taken for increasing drive power densities, with ~1 minute off-times between changing the power settings (see figure 8(*a*)).

The associated scanning rig was made from Time and Precision square section tubular construction frame, with a single carriage which forms the main support for the devices used to scan the cleaning bath field. Motor-controlled movement is provided in the longitudinal, transverse and vertical directions, with a positional resolution of 5 μm. The whole system is controlled by a Windows PC, via an ISA interface (see references [4, 5]).

Attachment to the movable carriage is via a V-clamp. This accepts poles which in turn can be used to support a range of sensor devices. A pole length of 0.5 m would be required to position a sensor in the vertical middle of the tank. Acoustic emission sensors were strapped to appropriate poles for

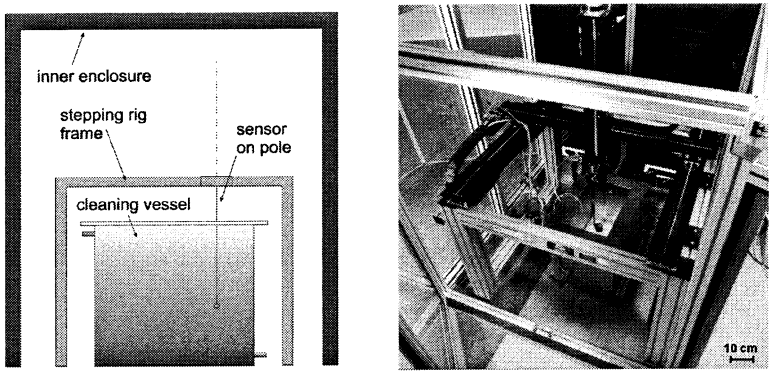

(a) *(b)*

Figure 3. (*a*) Schematic representation of bath, scanning rig and enclosure (not to scale). (*b*) Image (from above) of the test rig showing the automated positioning system, the test bath and the NPL PCS sensor placed within it on the end of a vertical mounting pole.

measurement. Sonochemical sensors used sample chambers made from the finger of a latex glove, assumed to be acoustically transparent at these frequencies (see section 2.2.2(*a*)). The latex finger (which contained 20-30 cm^3 of the sample) was immersed in the bath, and attached to a cylindrical glass tube of diameter 28 mm. Care was taken to ensure that the glass support did not enter the liquid, and that the sample being sonicated was completely submerged in the bath. This procedure was followed for the Weissler reaction, the Fricke dosimeter and the sodium terephthalate reaction, and a schematic of the arrangement is inset in figure 4.

The rig also provided a platform for a baseboard, from which various other sensors could be deployed. The baseboard contained a hole through which the CCD camera monitored the positions of the various sensors, and the locations from which sono- and chemi-luminescence were emitted. A test protocol was agreed between the authors, details of which can be found in reference [5].

As with the reference ultrasonic vessel, the reference medium was chosen and established by NPL prior to the COMORAC experiment [4]. From the results of the questionnaire performed in the information-gathering stage of the overall project, the majority of respondents who expressed a view said that they thought that aqueous media would be most appropriate, based on its ready availability, its versatility, and the fact that it is commonly used in industrial practice. Taking this, and also investigations at NPL to test the reproducibility of cavitation activity in different aqueous-based media (using the prototype

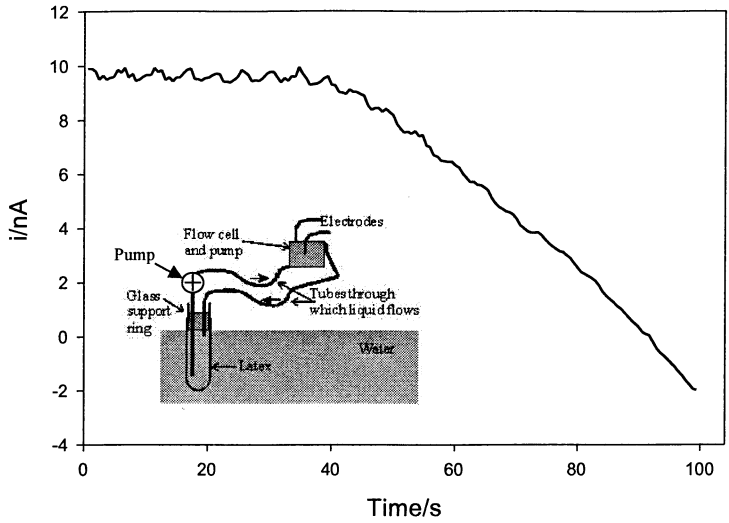

Figure 4. This figure shows the current versus time plot achieved for the reduction of I_3^- during the Weissler reaction. The initial straight line from 0-40 seconds is due to the time delay for the reaction mixture to be pumped from the latex glove sample holder into the flow cell. The rate is calculated from the slope of the graph after the initial plateau. The inset shows the flow cell apparatus.

cavitation sensor (PCS), and conventional hydrophones), the NPL concluded that filtered, de-ionised water degassed to 1.5 – 2 ppm level of dissolved oxygen content (DO_2) in the temperature range 21-22.5°C was an acceptable reference medium for this COMORAC test. With this medium, the reference vessel performed consistently and, as discussed in section 1.4, the spectral signal as monitored by hydrophone gave results that were reproducible to ±12 % [4, 5]. In part, this performance aspect is governed by the response of the cleaning vessel. This is because liquid samples which are very refined (such as highly degassed, filtered water) contain substantially fewer nucleation sites for cavitation activity than do less refined liquid samples. They therefore present an acoustic impedance to the bath drive circuitry which can cause the vessel to overload, and indeed very highly refined samples performed unstably.

It should also be noted that after the COMORAC study had been performed, NPL conducted a careful study of the cleaning vessel and the PCS. This gave some insight into the changes in the environmental conditions occurring within the vessel, during the actual measurement process [27]. This involved testing 'a standard mix of water' (at ambient temperature and 2 ppm of dissolved oxygen (DO_2)), and exposing it to increasing power densities

whilst recording acoustic emission spectra. Its response was also then monitored as the power density was reduced in order to investigate the presence of any hysteresis effects, in addition to the effect of the operation of the test vessel on the solution characteristics. Figure 11 of reference [27] shows that, whilst the results obtained with increasing drive powers indicated marginally lower levels of cavitation activity than when the drive power was decreasing, when the random uncertainties (reflecting the repeatability) were taken into account, the indications were that there was little difference between the two sets of results[1].

2.2 Sensors

There is a wide variety of potential sensors, both in terms of the physical effect of cavitation that a device will measure (acoustic, chemical, erosive, biological, electrical, etc.), and also in terms of the temporal and spatial characteristics of the signal. Other issues include:

- real-time monitoring and post processing;
- versatility with respect to the medium that can be used;
- ease of use and requirement for specialised measuring devices;
- reversibility and hysteresis;
- invasiveness.

The issue of invasiveness needs clarification, because it has many facets. An item may be considered to be invasive with respect to affecting the cavitation it measures, or with respect to interacting with other sensors one might wish to use simultaneously. There are many ways by which the presence of a sensor invasively affects the cavitation. The introduction of the sensor may perturb the driving ultrasonic field [28]. If a physical presence needs to be inserted into the liquid, it is sensible to design the sensors such that the sound fields to which the sensing volume is exposed, are not significantly different from those which would be present were the sensor not in place. This requirement is reflected in COMORAC by the use of the latex sample holder (section 2.2.2), and the geometries of the PCS sensor [29] and the focused bowl hydrophone [10]. Other options include the use of acoustically-transparent windows which provide blackout in order to measure sonoluminescence from submerged liquid samples [30,31]. However even for such sensors as these,

[1]Note however that two different sensors can in principle measure different degrees of hysteresis, for a variety of reasons. Notably, they might be responding to effects produced by different cavitational mechanisms (see section 5). Even if the mechanisms relevant to both are the same, the measurements of hysteresis might differ because of sensors issues such as linearity and saturation.

which have been designed to be minimally invasive with respect to perturbing the driving field, their physical presence can affect the cavitation, for example via the distribution of cavitation nuclei. In general, anything in the design of the sensor which increases the surface area of contact between sensor and liquid can be seen as potentially increasing the invasiveness with respect to nucleation. This is illustrated by the 1850 studies of Berthelot [32], who undertook static tests of liquid samples. The sample was heated in a closed glass tube which was almost filled with liquid, the remainder of the volume being gas. On heating, the liquid expanded more than the glass, forcing the gas into the liquid, so that the latter filled the vessel. On cooling, the liquid adhered to the glass: since the liquid was thus restrained from contraction, tension was generated within it. The tension increased as the liquid cooled, until cavitation occurred. With this technique, Berthelot measured the 'tensile strength' of his water sample to be around 50 bar. However this value did not represent the tensile strength of the water *per se*. Rather, it reflects the invasive nature of the solid/liquid interface with respect to cavitation nucleation. This is because the crucial observation for our purposes was that the cavitation in Berthelot's experiments initiated at the walls of the tube, rather than in the body of the liquid. It was therefore the forces of adhesion between glass and liquid that were overcome, not the cohesion between the liquid molecules. This demonstrates an important point, that it is not the properties of the liquid *per se* that determine the maximum tension a liquid can sustain, but often the other bodies present within the liquid sample [18§2.1.2, 33]. Therefore even when the immersed components of any cavitation detector are minimally invasive to the sound field, the sensor can be invasive with respect to the cavitation beyond simple liquid displacement. Recalling that Berthelot's tests were static, the situation becomes more complicated in dynamic conditions: when the sensor does have an acoustic effect of its own, the boundary conditions at the solid/liquid interface can generate enhanced pressures exactly at the location where enhanced nucleation conditions have been introduced [28].

Of crucial importance in discussing sensors for cavitation is the consideration of exactly *what* is being measured. We do not measure cavitation *per se*, but rather the effects it produces. There are many forms of cavitation, but for the purposes of this report we shall consider the term to mean those forms of bubble activity associated with the production of physical effects such as cleaning. Hence whilst most forms of cavitation produce an acoustic emission, relevant acoustic sensors will be those which respond to a signal that is characteristic of a form of cavitation which has potential to clean (such a jetting or inertial cavitation).

Cavitation is a threshold phenomenon, and a given sensor might measure just that threshold (the 'onset' – or cessation – of cavitation) i.e. it would indicate whether or not cavitation was present. Alternatively it might measure

some form of cavitational 'activity'. To be useful as a measure of cleaning bath efficacy, this signal should increase as the 'cleaning potential' of the cavitation increases, whether through an increase in the number of events, or an increase in the 'cleaning ability' of each individual event.

Consider a fictional manufacturer of cleaning baths. This manufacturer might want to send samples periodically to be filled with the reference medium, and check that the output is as required from the given detector. The manufacturer could then judge his cleaning baths against competitors[2]. Alternatively, he might use a reference to check whether a design change enhances the cavitation, or to check possible faulty units. This would be a measure of 'activity'.

In contrast, another company might be producing some liquid product, using ultrasound to process the material as part of the manufacturing process (e.g. to produce crystallization [34-36]). This company might wish to avoid the effects of cavitation (which could, for example, oxidise a product). Hence the requirement here is to measure the threshold, and ensure that the ultrasonic field remains in the sub-cavitation regime when in operation.

Measures of thresholds and activity both therefore have their uses. However such measurements are rarely simple. If a 'cavitation threshold' is detected, the sensor must be critically assessed to ascertain whether this represents measurement of a threshold for detection, for nucleation, or for a step-change in cavitational activity. For its part, the measurement of 'cavitational activity' brings with it additional complications relating to linearity, saturation etc.

The various sensors used in COMORAC are each described in the following subsections.

2.2.1 Luminescence sensors

2.2.1(a) Multibubble sonoluminescence, MBSL (University of Southampton)

The light emission resulting from MBSL is recorded. In theory the greater the cavitation intensity, the greater the light output. Photon counts were recorded from different areas of the bath to quantify any inhomogeneities in the distribution of the source of this cavitation-induced emission.

Measurements were performed using an EG&G SPCM – 200 – PQ Photon counter module and an EG&G multichannel scalar (Model 914P) interfaced to a PC. The directionality and footprint of the photon counter (used for the tests of 2.2.1(*a*) and 2.2.1(*b*)) were estimated as indicated in figure 8(*b*) (noting however that the footprint will be dependent on the signal-to-noise ratio

[2]although this strictly would be judging their effectiveness at producing whatever effect it is that the detector responds to, in the given medium only – hence the requirement, stated above, that the effect measured in some way reflect the 'cleaning potential'.

(SNR)). Image-intensified photography and video in principle provide a more rapid assessment of inhomogeneity (although without the same degree of objective quantification). In COMORAC the SNR only made such imaging possible for the sonochemiluminescence tests of section 2.2.1(*b*).

2.2.1(b) Sonochemiluminescence (University of Southampton)

An alkaline solution containing luminol (triaminophtalhydrazine) is irradiated with power ultrasound. This solution, in the presence of a strong oxidising agent, is known to emit light through a complex chemiluminescent reaction [37]. The oxidising agent in this case is presumed to originate from the generation of hydroxyl radicals. It is assumed that the greater the 'cavitational activity' (see section 2.2), the greater the associated light emission. Light emission was recorded in different regions of the bath.

Chemiluminescent pictures are taken to image the sound field and to identify the chemically active and inactive zones in the bath. These are refereed to as 'hot' and 'cold' spots respectively. The chemiluminescent pictures were captured and recorded using a Darkstar image intensified CCD camera from Photonic science and a Nicam video recorder respectively. Quantified light emission measurements were recorded using a photon counter as described in section 2.2.1(*a*).

2.2.2 Sonochemical sensors

2.2.2(a) Weissler reaction (University of Southampton)

A standard solution of potassium iodide (KI) is sonicated. Oxidising species produced by cavitation convert I^- to I_3^- [38]:

$I^- + OH^\bullet \rightarrow OH^- + I^\bullet$ reaction (1)

$I^\bullet + I^- \rightleftarrows I_2^{\bullet-}$ reaction (2)

$2I_2^{\bullet-} \rightarrow I_2 + 2I^-$ reaction (3)

$I_2 + I^- \rightleftarrows I_3^-$ reaction (4)

COMORAC introduced a new way of following this reaction: rather than discontinuous sampling of the sample through the removal of aliquots for spectrometric analysis, the reaction was followed electrochemically by reducing the product of the reaction (I_3^-) to I^- at a platinum electrode [39]. The tri-iodide concentration was measured by chronoamperometry using a platinum working electrode (see below). The follow reduction reaction occurs at the electrode surface at the mass transfer limited[3] steady state:

[3]'Mass transfer limited' conditions occur if the potential of the working electrode is such that any species arriving at the surface of the electrode is immediately

$I_3^- + 2e \rightarrow 3I^-$ reaction (5)

Using the pump calibration, the rate of I_3^- production at a given irradiation frequency was determined by applying equation (1):

$$\frac{dc}{dt} = \frac{-1}{nFAk_m}\left(\frac{di}{dt}\right) \quad \text{equation (1)}$$

In this expression *dc/dt* is the rate of tri-iodide production in mol dm^{-3} s^{-1} (where *c* is the concentration in moles dm^{-3}), *n* the number of electrons involved in the electrochemical reaction, *F* is Faradays constant, *A* the electrode area, k_m the mass transfer coefficient within the flow cell and *di/dt* is the slope of the current versus time plot. Figure 4 shows a typical response recorded in the COMORAC exercise.

In order to make these measurements, a sample of KI was placed in an acoustically transparent container in the bath (a finger of latex glove; see inset of figure 4, and section 2.1). A flow cell was set-up in conjunction with a peristaltic pump that pumped liquid from the acoustically transparent container into the electrochemical cell during the experiment. The I_3^- concentration was determined using a 0.5 mm diameter Pt microelectrode as a working electrode. The potential applied to the working electrode was +0.2 V *vs.* Saturated Calomel Electrode (SCE). The slope of the current against time plot can be used to determine the rate of this reaction. A potentiostat (constructed in-house) was employed to control the potential of, and output the current from, the electrochemical cell. The electrochemical signal was then recorded onto a PC via an ADC card interfaced using in-house written software.

2.2.2(b) Hydroxyl radical production: The terephthalic acid (TA) dosimeter (University of Bath)

A standard solution (0.005 mol dm^{-3}) of terephthalic acid in dilute (0.05 mol dm^{-3}) aqueous sodium hydroxide solution was sonicated. Hydroxyl radicals ($OH^\bullet$)

---

electrochemically consumed (e.g. oxidised or reduced). If the electrolyte around the electrode is stationary, then the rate at which species travel to and from the electrode is usually controlled by diffusion alone. As the reaction progresses in a still solution, a diffusion boundary layer builds up around the electrode. Under these conditions, the population of the chemical species on which the reaction at that electrode is based, becomes depleted. Flow in the liquid (due to convection, streaming, turbulence etc.) can disturb this boundary layer and refresh the depleted population there. This enhances the rate of this type of electrochemical reaction, and hence augments the current recorded at the electrode.

are formed from the sonolysis of water and these radicals are trapped to form highly fluorescent 2-hydroxyterephthate ions, HTA (figure 5). Its formation is monitored by fluorescence spectroscopy.

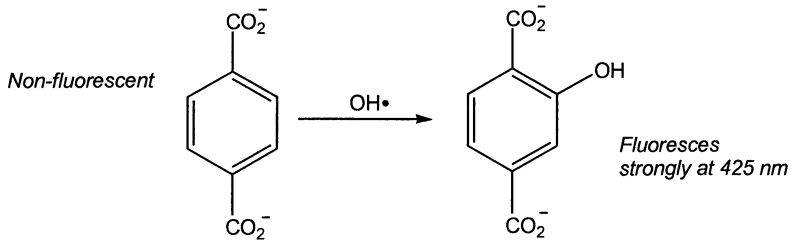

Figure 5. Schematic of the reaction in which, during sonication, hydroxyl radicals (OH•) formed from the sonolysis of water are trapped to form 2-hydroxyterephthalate ions.

In principle, as the cavitation activity increases within the sample, HTA will be formed and the fluorescence signal will increase. For a 22 kHz drive frequency, Price and Lenz [40] found a linear dependence of the signal as a function of acoustic drive intensity, measured calorimetrically, up to a certain point (~40 W cm^{-2}) after which the signal was found to tend to a plateau. The method is highly sensitive, with sub-micromolar amounts of $OH^{\bullet}$ being detectable.

Associated apparatus includes a fluorescence spectrometer (13A power source required) and the chemical solutions. The acoustically transparent container (the finger of the latex glove shown inset in figure 4, though without the electrochemical flow cell attachment) was positioned at the 'hot' spot as indicated by luminescence measurements. Into this container was placed a 30 cm^3 volume of the TA solution. The increase of fluorescence was monitored with time at various drive powers of the bath. Fluorescence intensity was measured using excitation and emission wavelengths of 310 nm and 425 nm respectively.

2.2.2(c) "Fricke" dosimeter (University of Bath)

This dosimeter is adapted from that long established for use with ionising radiation. A standard solution of ferrous (Fe^{2+}) ions is sonicated. Cavitation causes oxidising species to form from sonolysis, which in turn convert Fe^{2+} to Fe^{3+} [41]. The two ions have different absorption spectra and so can readily be monitored using spectrophotometry. A complex reaction sequence takes place including:

$OH^{\bullet} + Fe^{2+} \rightarrow Fe^{3+} + OH^{-}$ reaction (6)

$H^{\bullet} + O_2 \rightarrow HO_2^{\bullet}$ reaction (7)

$Fe^{2+} + HO_2^{\bullet} \rightarrow Fe^{3+} + HO_2^{-}$ reaction (8)

$HO_2^{-} + H^{+} \rightarrow H_2O_2$ reaction (9)

$Fe^{2+} + H_2O_2 \rightarrow Fe^{3+} + OH^{\bullet} + OH^{-}$ reaction (10)

In COMORAC, spectrophotometry is used to measure the concentration of Fe^{3+} in aliquots removed from the test solution at equal intervals. From this the rate of production of Fe^{3+} is calculated. Since COMORAC, the electrochemical technique for continuous monitoring, shown in figure 4 and used in COMORAC to monitor the Weissler reaction, has been adapted to monitor the Fricke reaction as well [26]. For a 22 kHz drive frequency, Price and Lenz [40] found a linear dependence of the signal as a function of intensity, measured calorimetrically, up to ~30 W cm^{-2}.

Associated apparatus includes a UV spectrophotometer (13A power source required). The experiments were conducted in the same manner as those with terephthalic acid (see section 2.2.2(*b*)).

Unless a calibration is performed specifically using the effective yield of the dosimeter employed under the solution conditions used[4] [42], the results of the TA and Weissler sonochemical dosimeters discussed above can only be expressed in arbitrary units or as a chemical rate. However, whilst the Fricke dosimeter could also be calibrated in this way, it has in addition features which offer perhaps a more transportable option. Specifically, it has a well documented yield per equivalent dose of ionizing radiation, a relatively simple composition and does not require spectrometer calibration (through synthesis of 2-hydroxyterephthalic acid). Hence this dosimeter can be used to compare the effect of cavitation directly with ionizing radiation. This comparison, using an electrochemical detection technique, has been made elsewhere [39]. To accomplish this, it is appropriate to consider an equivalent dose to which the solution is subjected by cavitation. The equivalent dose rate (Rads s^{-1}) can be calculated from standard dosimetry texts and requires the rate of absorbance change determined from the experiments and equation (2):

$$D_{rads} = \frac{N_A[\Delta A]}{10(\Delta\varepsilon)G(Fe^{3+})f\rho l} \qquad \text{equation (2)}$$

[4]It has been shown [42] that the $OH^{\bullet}$ yield (determined as a G value in mol J^{-1} using an optimised TA dosimeter) can vary as a function of ultrasonic frequency, position within the vessel and ultrasonic power.

where D_{rads} represents the dose in rads, N_A Avagadro's number, ΔA the change in the absorbance (A) of the solution, $\Delta\varepsilon$ the difference in the extinction coefficients of Fe^{2+} and Fe^{3+}at the appropriate wavelength, $G(Fe^{3+})$ represents the yield of Fe^{3+} for 100 eV, f =6.24 x 10^{13} eV rad^{-1}, ρ is the density of the media and l is the optical path length [41]. Indeed as the results of a multiple set of measurements were recorded under similar conditions, this enables an equivalent dose to be attributed to the measurements obtained with the other systems (see figure 24(a)).

2.2.2(d) Calorimetry (University of Coventry)

As a measurement technique, calorimetry differs from the other sensors deployed in COMORAC in that it does not measure a cavitational effect. Rather, it is the most commonly used method amongst chemists to measure the amount of ultrasonic power entering a sonochemical reaction. It involves measurement of the initial rate of heating produced when the system is irradiated by power ultrasound.

Ideally the method should use specially designed calorimeters of which there are two types: adiabatic (or quasi-adiabatic calorimeters) and non-isothermal, non-adiabatic calorimeters (often referred to as n-n calorimeters). The accuracy of measurements made using such methods will increase if:

- all the acoustic energy entering the system is transformed into heat; this requires good matching of the system and low reflections at any interfaces;
- the temperature measurements are very accurate; temperature rises are greater at high intensities and this will also generally require that the time response factor of the thermometer must be rapid.

This is a simple method of estimating the overall acoustic power entering a reaction even when a thermally insulated vessel is not employed. For this reason a chemist will normally use the vessel in which the reaction is being performed to produce an approximation to the true energy input.

For the system under study the temperature (T) is recorded against time (t), at intervals of a few seconds using a thermocouple placed in the reaction itself. From the time history of T, the initial temperature rise (dT/dt as $t \rightarrow 0$) is then estimated. This is achieved either by constructing a tangent to the curve as $t \rightarrow 0$, or by curve-fitting the data to a polynomial. That component of the ultrasonic power (W) which is converted at a given rate into heat (W_T) can then be obtained from the product $W_T=(dT/dt)c_pM$, where c_p is the heat capacity of the solvent (J $kg^{-1}K^{-1}$) and M is the mass of solvent used (kg).

If the rate of conversion of acoustic energy into heat is assumed to be equal to the acoustic power emitted by a source of area A, then the acoustic intensity can be estimated by consideration of the ratio of W_T to the area normal to the flow of power.

2.2.3 Acoustic sensors

2.2.3(a) NPL broadband passive acoustic sensor (PCS)

The COMORAC study used an early pre-prototype version (the only version available at the time) of the NPL broadband sensor that was developed as part of a Strategic Research programme at NPL. This type of sensor utilizes a thin film of pvdf (polyvinylidene fluoride) to detect the broadband acoustic emissions generated by cavitation. Novel features of the sensor are a hollow cylindrical shape, which endows the sensor with a degree of spatial resolution. Signals of interest lie in the frequency range 1.5 to ~10 MHz. The concept, design and early performance evaluation of the prototype has been fully described in two papers published following COMORAC [27, 29]. The sensor used in COMORAC differed from the sensor described in these papers in a number of respects, most important of these being the protection of the electrode. In the final version such protection is provided by a thin layer of rubber (of thickness 0.4 mm) whose acoustic impedance is closely matched to that of water [29]. The sensor electrodes used during COMORAC had only a thin layer of primer to protect them from cavitation within the vessel, which made them susceptible to erosion. Discovery of this susceptibility was an important outcome of the COMORAC trial and motivated the subsequent refinement of the device: COMORAC's PCS sensor was used in many of the tests for cross-calibration, and so was subjected to the sort of prolonged erosive exposures which a practical cavitation sensor might encounter, but to which many putative 'cavitation detectors' are rarely exposed in their testing phase. The post-COMORAC sensor has subsequently seen extensive use [27, 29, 43-47].

The spectra from both the PCS and the focused bowl device (see section 2.2.3(*b*)) were analyzed in the same way to obtain a single numeric from a given drive setting of the cavitation bath[5]. The reference power for the dB

[5] When plotting a spectrum from the voltage time history output of a sensor, there are a number of conventions. With the frequency usually plotted on the abscissa, the four most common options for the mantissa are: V Hz^{-1}; V^2 Hz^{-1}; V; V^2. Clearly the representations that use V^2 in preference to V are plotting a parameter which reflects the energy of the signal, as opposed to the amplitude. The advantage of using Hz^{-1} comes from the common interpretation of a spectrum is as a histogram, since the frequency bins will be finite: changing the width of these bins should affect the amplitude of the spectral level plotted. This is certainly appropriate for broadband signals. However this is problematic if the signal is a sine wave. For a sine wave, the

scale in the spectra was 1 mW, such that (with a 50 Ω input impedance to the spectrum analyser) the voltage corresponding to 0 dB is $\sqrt{50\times10^{-3}} \approx 0.2236$ V. The squares of the relevant voltages were integrated over a specific frequency band, from 1 to 5 MHz for the PCS. Two options were used for the focused bowl device: the 'peak' energy was integrated from 1.07 to 1.09 MHz; the 'broadband' signal was based on an integration from 0.87 to 1.27 MHz. Such integrations, for both PCS and focused bowl devices, convert the relevant portion of each spectrum into a single representation of 'cavitation activity', the units of which are Volts squared Hertz (i.e. effectively, power). This is plotted in figures 16-18 as a function of the power density of the driving field. The procedure is described more fully in references [27, 29].

2.2.3(b) Focused bowl passive acoustic sensor (Guy's and St Thomas' Health Trust)

This device utilises a 10 cm diameter focused bowl hydrophone, with a nominal 1 MHz resonance, as a passive device to detect acoustic emission from cavitation at this frequency. The equipment consists of the 10 cm diameter focal bowl, filter and data acquisition [10,11]. The focal bowl can be semi-immersed in water but is normally used with a water-filled adapter that has an acoustic window. For COMORAC, the hydrophone output was processed in the manner described in section 2.2.3(*a*). The device is not calibrated.

2.2.3(c) Cavitation Activity Indicator IC-3 (Belarus State University)

One of the instruments tested in COMORAC was the 'Cavitation Activity Indicator IC-3'. It was developed as part of an AEU INTERS programme and is intended for cavitation activity measurements. Details are restricted for commercial reasons. The apparatus is based on analysis of the spectrum of cavitation noise in the frequency range 5 kHz-10 MHz. It does this in a number of ways, the method of prime importance for COMORAC being measurement

---

energy in the bin is independent of the bin width, since all the energy is at a single frequency, i.e. it has zero bandwidth. Only one of the bins will contain non-zero energy. Division of the energy of that bin by the bandwidth of the bin simply causes the spectral peak corresponding to the sine wave to reduce in amplitude as the bin width increases. As a result, the parameters V and V^2 are sometimes used in preference to V Hz^{-1} and V^2 Hz^{-1}, if the signal is perceived to more closely resemble a sinewave than a broadband signal. It is this latter convention that was used to analyse the focused bowl and PCS sensors in COMORAC. As a result, when the area under the spectrum is calculated to produce the quantities on the mantissas of figures 16-18, the quantity is $V^2Hz = V^2s^{-1}$, a quantity resembling power.

of the intensities invested in the subharmonic of the driving frequency. It uses a wide-band hydrophone protected against cavitation effects, and is suitable for measuring the cavitation which results from driving fields having a frequency range from 5 kHz to 150 kHz. The apparatus is multifunctional and is intended for the following measurements:

- Total bubble activity;
- Transient bubble activity;
- Subharmonic intensity;
- Integral hydrophone output;
- Fundamental frequency of the driving field.

This sensor travelled by far the longest distance to get to NPL for the COMORAC test, and suffered most abuse on the journey, which damaged some of its components. During the COMORAC study, only the subharmonic feature of this system was operational.

2.2.4 Erosion sensors

2.2.4(a) Polymer degradation (University of Bath)

When a solution of a long-chain polymer dissolved in a solvent is sonicated, extensional flows around cavitation bubbles and in microjets result in chain breakage. The degree of breakage is a measure of cavitational activity and can be found by measuring the molecular weight of the polymer.

A sample of 30 cm^3 of a 1 g dm^{-3} solution of dextran (a soluble polysaccharide obtained from Fisher) was sonicated using the same method as used for the other solutions. Sonication was carried out for 10 minutes at each drive power level. Polymer molecular weights were measured using size exclusion chromatography. The extent of degradation can be measured from the average number of chain breaks, N_c given by equation (3):

$$N_c = \left(\frac{M_n(0)}{M_n(t)} - 1 \right) \qquad \text{equation (3)}$$

where $M_n(0)$ is the number average molecular weight before sonication, and $M_n(t)$ is the number average molecular weight after some sonication time t.

2.2.4(b) Particle erosion (University of Bath)

Another potential measure of cavitation is the modification of the particle size and distribution of solid particles suspended in a cavitating liquid. The change in particle size is a well known sonochemical phenomenon [48]. Changes depend on the properties of the solid: particles of softer metals fuse

together to increase the average size, while those of hard, brittle metals fracture to give smaller particle sizes. Similar behaviour has been described for solid polymers suspended in water, and the extent of the change has been shown to depend on the sound intensity used [49]. The chemical modification of solid surfaces also depends on the sound intensity and therefore, presumably, on the 'amount' of cavitation [50]. Since COMORAC, these effects have been investigated further in metal powders [51].

Although it was not expected to be a widely applicable method owing to the measurement methods, it was felt worthy of preliminary evaluation. Particle sizes are most easily determined by light scattering or by microscopy, neither of which is straightforward in routine application.

As an initial attempt, polystyrene spheres with a diameter 10 – 20 μm were used in water. However, difficulties were encountered in distributing the solid through the water at the intensities available in the reference cavitation vessel. The solid particles formed clumps and could not be formed into an even suspension. The time constraints of COMORAC meant that it was not possible to experiment on attempting to achieve dispersal using detergents/solvent etc. without sacrificing another test, and so the attempt to achieve a sensor based on particle erosion was abandoned. Therefore, no results for particle erosion were recorded.

2.2.4(c) Electrochemical erosion (University of Southampton)

The electrochemical detection of individual erosion events, as the result of erosive mechanisms produced by cavitation, has been reported previously by Birkin *et al.* [52]. In this technique a passivated electrode was held under electrochemical control and placed within the plume of an operating ultrasonic probe. Erosion of the passivating surface caused a corrosion process to be initiated on the surface of the electrode. This corrosion process was driven by the electrochemical control held over the sensor employed. Hence for each erosive event that occurred over the surface of the electrode (125 μm diameter Pb), an anodic current was observed. Figure 6 shows a current time history for such a system recorded in this manner. In an effort to explore this system as a possible cavitation sensor an array of electrodes was fabricated.

Three 0.5 mm silver electrodes, set in epoxy resin, were attached together to form a vertical array. Each electrode was positioned at a different height. The electrodes were held at a potential at which silver iodide formed on the surface. In this way a passivating film is formed on the surface. Cavitation removed the passive silver iodide film. The exposed surface, which is held under electrochemical control, re-oxidised in response to the erosion as a result of inertial cavitation processes. The bath was employed as a reference/counter electrode in this experiment. Each electrode will in theory yield information about inertial cavitation occurring in that region of the bath. By the time of the

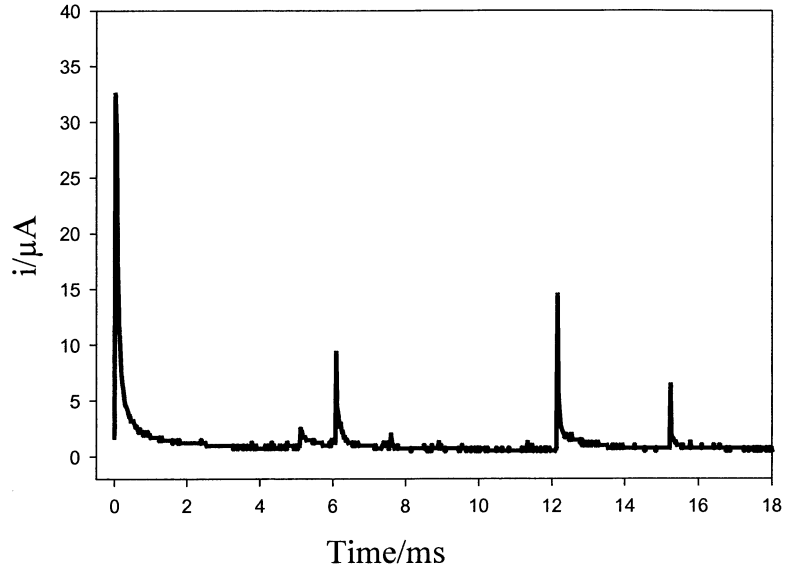

Figure 6. Current time trace recorded for a passivated 125 μm diameter lead electrode exposed to ultrasound (22.5 kHz, 92 W cm^{-2}) [52]. Each erosion event is detected as an anodic reoxidation transient as the surface 'heals' itself back to the passive state. The charge associated with each event is a measure of the degree of surface damage as a result of each cavitation event.

COMORAC trial, only a pre-prototype device was available and it did not generate useful results. Following COMORAC, and partly as a result of the experience of COMORAC, a working system has been developed [52-54].

2.2.4(d) Foil erosion (NPL)

Sheets of aluminium foil were placed on thin wire frames and immersed in the bath. Visual inspection clearly indicated that cavitation erosion of the foil had occurred preferentially close proximity to the frame, rather than reflecting the 'hot' and 'cold' spot distribution (section 3.1). Hence the instrument, as it was designed, was too invasive to provide useful data. The lack of success was in part because of the reputation that foil erosion has achieved as being a simple-to-use technique. Because of this, in prioritising tasks within the time constraints that were the defining characteristic of COMORAC, the time

allotted to testing the foil erosion sensor proved to be insufficient to allow the degree of refinement which we now believe the sensor requires. Such refinements are necessary to ameliorate the invasiveness problem to a degree which would allow usable results to be taken.

COMORAC showed that, whilst erosion results could be obtained, these reflected the geometry of the frame used in COMORAC rather than the unperturbed cavitation field. Having learnt from COMORAC that more time needs to be spent in expert design of a foil erosion system, such a sensor has been successfully constructed and compared with the results of the modified version of the PCS sensor (the one which contains greater erosion resistance than that used in COMORAC) [55].

3. Results

3.1 Luminescence sensors

Table 1 shows the order in which the tests were undertaken. It was important that the spatial distribution of chemiluminescence (figure 7) was measured first, because of the differing footprints, spatial resolutions and averaging inherent in the sensors employed. Only this could produce a time-resolved map out the simultaneous activity in the bath and, as figure 7 shows, this proved to be inhomogeneous. Regions of high and low activity (termed 'hot' and 'cold' spots respectively) were identified with this technique, vital information given that some of the sensors had footprints of dimension ~1 cm^2. In addition, it allowed real-time monitoring of any modifications in cavitation activity (amount, distribution, stability etc.) which occurred resulting from the insertion of sensors (latex finger, foil etc.) into the bath (figure 7).

Comparing in figure 8(*a*) the sonochemiluminescent photon counts obtained during the on-times of sonication, with the background counts detected during the off-times (during which the power setting were changed), note that there appears to be no threshold for the onset of sonochemiluminescence in these measurements. However physically we know that such a threshold must exist, and hence deduce that here it must occur at power density settings of <2.5 W dm^{-3}). Note also that there appears to be a change in the gradient of the emission versus drive power density when the latter equals ~10 W dm^{-3}. This value may be postulated to be a threshold for enhanced activity.

The photon counter produced time histories of which figure 8(*a*) is typical, for sonication as the drive volumetric power density was increased in time. The footprint is small enough (figure 8(*b*)) to distinguish between the 'hot' and'cold' spots (figure 9). It should be emphasised that because of the possibility of hysteresis, plots such as figure 9 were taken not just for increasing

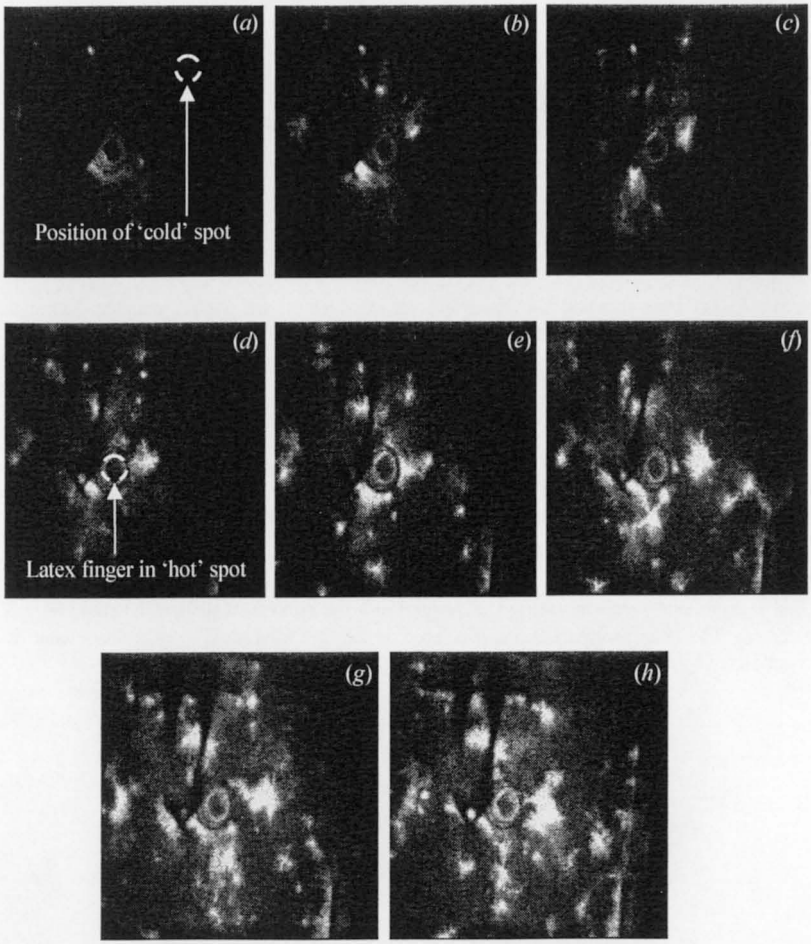

Figure 7. Sonochemiluminescent pictures recorded from above the ultrasonic bath as a function of the volumetric power density. The volumetric power density increases respectively from picture (*a*) to (*h*). The power settings were 2.5, 5, 7.5, 10, 20, 32.5, 42.5, and 47.5 W dm^{-3} respectively. The temperature of the bath was 21°C. The height of the camera above the surface of the 18 litre luminol solution was 45.5 cm ± 1 cm. The circle in (*a*) has a diameter of 2 cm and demarcates the 'cold' spot. The circle in (*d*) is aligned with the cross-sectional perimeter of the latex finger at the 'hot' spot. In the other frames luminescence or scattered light is visible from this perimeter. The centres of the 'hot' and 'cold' spots are 89 mm apart.

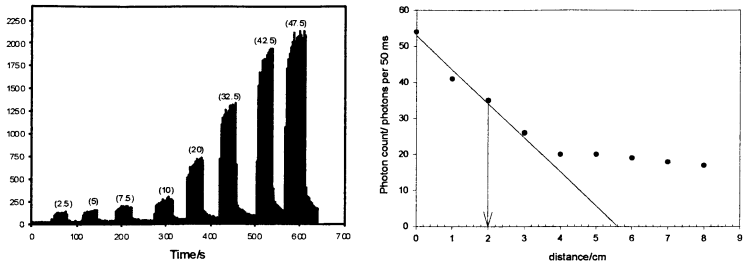

Figure 8. (*a*) Plot showing the raw data recorded from the photon counter during a sonochemiluminescent experiment. The ultrasonic irradiation in this case was chopped on and off while the volumetric power density (shown in parenthesis, units W dm^{-3}) was increased in a step-wise fashion as time progressed. (*b*) Prior to COMORAC, the footprint of the photon counter was determined several times by placing the counter 10 cm above a Beta light point source, and then measuring the mean photon count at a series of positions by moving the light source with respect to the detector. The distance off-axis until the count was 50% of the peak (arrowed) was 2 cm ±5%, and the distance until the count reached the background level was 4 cm ±3%. When used in COMORAC, the photon counter was 18 ± 0.5 cm above the liquid surface. Hence, for similar signal-to-noise conditions, this detector's footprint on the water surface for demarcating a 50% count would have a radius of 3.6 ± 0.2 cm, and for demarcating 0 dB signal-to-noise conditions the radius would be 7.2 ± 0.3 cm. The latter footprint limits, if centred on the 'hot' and 'cold' spots (whose centres are separated by 8.9 cm), would overlap (figure 7).

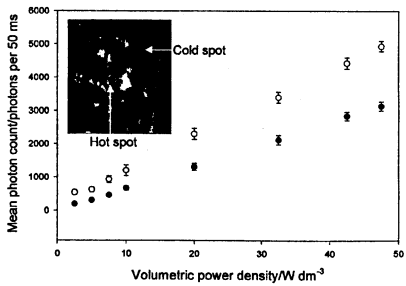

Figure 9. This figure illustrates the mean photon count recorded from a luminol solution with the photon counter positioned directly above a 'hot' or 'cold' spot. The 'hot' spot and the 'cold' spot are represented by the (○) and (●) respectively (although the degree of localisation is much less than for the 2 cm diameter latex finger – see figure 8(*b*)). In the case of the 'hot' spot the temperature ranged from an initial value of 21.6°C to finally 22.8°C. The height of the photon counter above the solution surface was 18 ± 0.5 cm in both cases. In the case of the 'cold' spot measurements the initial temperature was 22.5°C while the final temperature was 23.4°C. The error bars represent ± one standard deviation from the mean photon count (averaged over 20 s of data).

power densities, but also for decreasing and randomised settings of the tank drive level (figure 10). In addition to the images and measurements recorded for the sonochemiluminescent experiments, luminescent measurements were attempted employing direct measurement of MBSL output of the standard tank. Figure 11 shows the mean photon count recorded as a function of the power setting employed. Clearly an increase in photon count is apparent, but the error bars indicate that this method is prone to inaccuracies due to the low signal to noise ratio measured in this experimental arrangement. Note also that since light emission was detected under similar conditions in the sonochemiluminescence experiments (see figure 8(*a*)), it is likely that the absence of a signal <20 W dm^{-3} in figure 11 is the result of the low signal to noise ratio produced in these experiments. Hence there is a detection threshold at <20 W dm^{-3} for this system.

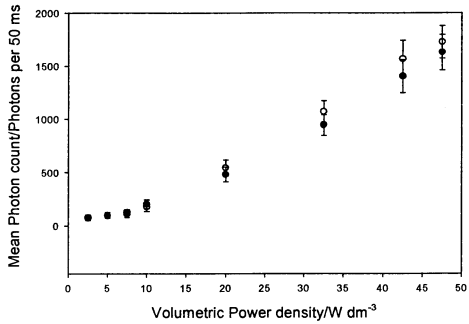

Figure 10. The sonochemiluminescence of a luminol solution recorded when the detector is placed (in plan view) over the geometric centre of the bath. Measurements were performed in both the forward and the reverse direction at the different powers respectively. The open circles (○) represent the forward scan (i.e. increasing drive power density) and the (●) represents the reverse scan (i.e. decreasing drive power density). Initially the temperature was recorded as 20.8°C while at the end of the experiment it had been raised to 21.7°C. The height of the photon counter window above the surface of the water was 20 ± 1 cm. Note there were no DO_2 measurements recorded in this case as the sensor was not compatible with the conditions employed. The error bars represent ± one standard deviation from the mean photon count (averaged over 20 s of data).

3.2 Sonochemical sensors

Figure 12 shows the results obtained for the Weissler reaction in the 'hot' spot as a function of volumetric power density compared to a single measurement in the 'cold' spot at 47.5 W dm^{-3}. The latex pocket confines the sonochemical tests to a circular 'footprint' (of diameter ~2 cm), outside of

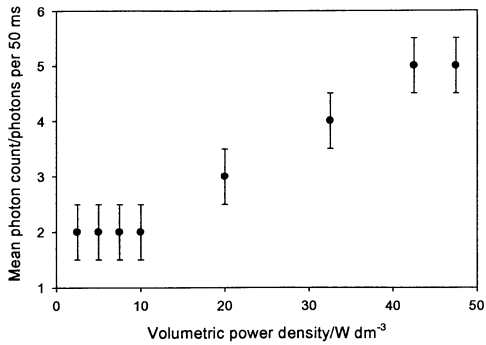

Figure 11. Plot showing the mean photon count recorded from a 18 litre solution of water with the photon counter positioned in the region of the 'hot' spot. The initial dissolved oxygen was 3.91 ppm and the temperature was 25.5°C. The height of the photon counter above the surface of the water was 22.5 ± 0.5 cm. The final dissolved oxygen was 4.44 ppm and the temperature was 26.5°C. The error bars represent ± one standard deviation from the mean photon count (averaged over 20 s of data).

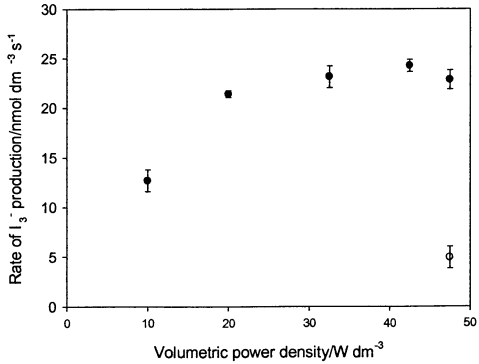

Figure 12. Plot showing the rate of I_3^- production (Weissler reaction) (•) in the 'hot' spot determined using the electrochemical flow cell technique as a function of the volumetric power density. In addition the rate was determined in the 'cold' spot at 45 W dm^{-3} (○). In all cases 20 cm^{-3} of 100 mM KI were placed in the latex finger. The initial and final liquid temperatures were 21.2°C and 22°C respectively. The error bars represent the 95% confidence interval determined from linear least mean square analysis of the current time data obtained. The measurements were recorded sequentially from low to high power density. The initial and final DO_2 measurements during this experiment were 10.22 ppm and 13.22 ppm respectively. Whilst the authors have decided to retain the values of DO_2 obtained from the instrumentation, we note that these two values appear to be anomalously high.

which there is no possibility of signal collection. Hence figure 12 shows that the Weissler sensor is in this case more sensitive than imaging luminescence, which in figure 7 produced no signal from the 'cold' spot. The Weissler reaction, on the other hand, shows a 'cold' spot signal at 47.5 W dm^{-3} drive power that is less than that obtained at the 'hot' spot when the drive power was 10 W dm^{-3}. That photon counting produces a 'cold' spot signal which is ~30 W dm^{-3} the corresponding 'hot' spot one at 47.5 W dm^{-3} drive power (figure 9) reflects the fact that its footprint is not only larger, but has a 'soft' boundary (see figure 8(*b*)).

Figure 13 shows the results of the "Fricke" dosimeter (the oxidation of $Fe^{2+} \rightarrow Fe^{3+}$). It shows the rate of Fe^{3+} production as a function of the volumetric power density applied to the bath. The rate was calculated from the

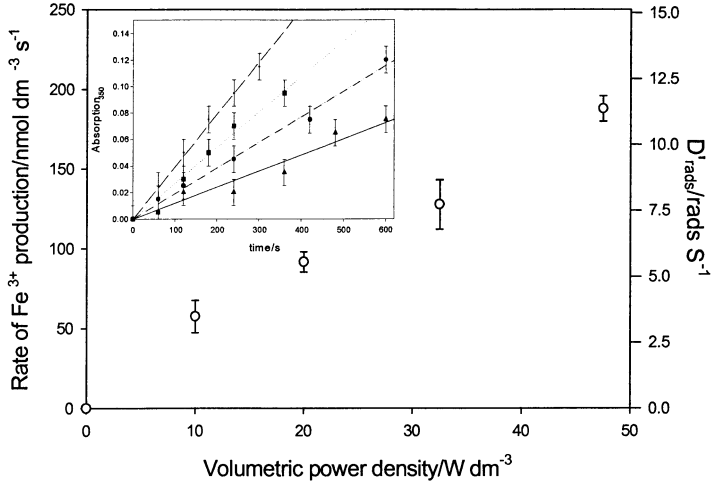

Figure 13. Plot showing the rate of Fe^{3+} production as a function of volumetric power density. The insert shows the actual absorbance readings, at an optical wavelength of 350 nm, as a function of time for each power setting employed (▲, ●, ■ and □ for 10, 20, 37.5 and 47.5 W dm^{-3} volumetric power densities respectively). The error bars on the insert are estimated from the accuracy of the spectrometer employed. The main plot shows the equivalent dose calculated from the insert. In these calculations the molar extinction coefficient at an optical wavelength of 350 nm takes a value of $\varepsilon_{350} = 2100$ dm^3 mol^{-1} cm^{-1}. The error bars in the main plot represent the 95% confidence interval determined using the data from the linear regression for each power setting in the insert. The measurements were recorded with the sample holder placed in the 'hot' spot determined by luminescent imaging (see figure 7). The temperature rose from an initial value of 22°C to 30°C during these experiments.

change of absorbance at 350 nm in the UV/Visible spectrum (shown in the inset for the various power settings). Since the Fricke reaction can also be used to characterise ionizing radiation (section 2.2.2(*c*)), it is possible to attribute on this figure the equivalent dose in rads s^{-1} which the power ultrasound produced on the sample within the latex finger.

Whereas the Fricke dosimeter is a measure of a number of oxidising species produced by cavitation in solution, the terephthalic acid (TA) dosimeter is specific in responding to hydroxyl radicals. The rate of radical production, given by the rate of increase of fluorescence, rises with increasing drive power as shown in figure 14. However, unlike the Fricke dosimetry results, there is a maximum power after which it is assumed that less of the product (2-hydroxyterephthalic acid) is produced (see section 4.1).

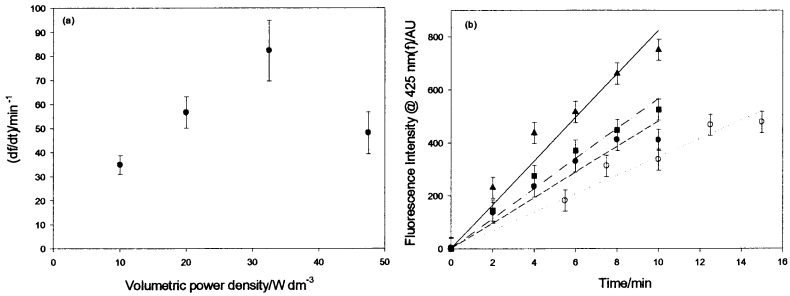

Figure 14 (*a*). Plot showing the dependence of the rate of HTA production as a function of the applied power. These rates are calculated from a linear fit to the time history of the fluorescence emission from HTA (see part (*b*)) formed by sonication at various power densities. The initial and final liquid temperatures are 23°C and 24.6°C respectively; the initial and final DO_2 readings are 2.84 ppm and 3.62 ppm respectively. The error bars in (*a*) represent the 95% confidence interval determined using the data from the linear regression for each power density setting shown in part (*b*) (*i.e.* 10 W dm^{-3} (o), 20 W dm^{-3} (■), 32.5 W dm^{-3} (▲) and 47.5 W dm^{-3} (●)). The error bars in (*b*) are estimated from the accuracy of the spectrometer employed.

3.3 Acoustic sensors

During COMORAC it was possible to obtain publishable results comparing the 'hot' and 'cold' spot signals for several sensors, e.g. sonochemiluminescence and Weissler reactions. For other sensors, the time constraints of COMORAC did not allow 'cold' spot data to be taken. Of the

three acoustic sensors, the focused bowl could not be present to take 'cold' spot data on the second day of its scheduled test, because of national petrol strikes. By the time the PCS sensor was deployed at the cold spot, the cumulative erosion damage made it unworkable. However, following the upgrade of the PCS sensor subsequent to COMORAC, not only did the PCS sensor perform far more reliably, but there was time to complete a comparison of its detection performance in both the 'cold' and 'hot' spots. The malfunction of the other features on the IC-3 device freed up time to use its subharmonic sensor to explore, not only the 'cold' spot, but also the vertical inhomogeneity of the 'hot' spot.

The spectra measured with the focused bowl hydrophone are shown figure 15 for the 'hot' spot. From these data, two parameters are extracted and plotted in figure 16 against volumetric power density: the broadband noise in the spectrum and the energy contained in the peak of the spectrum (in range 1.07-1.09 MHz). Without error bars it is impossible to assess the significance of the plotted reduction in peak energy at the highest drive setting, compared to the plotted monotonic increase in the broadband signal (although of course a mechanism for such an outcome, if it existed, could be attributed to increasing nonlinearity).

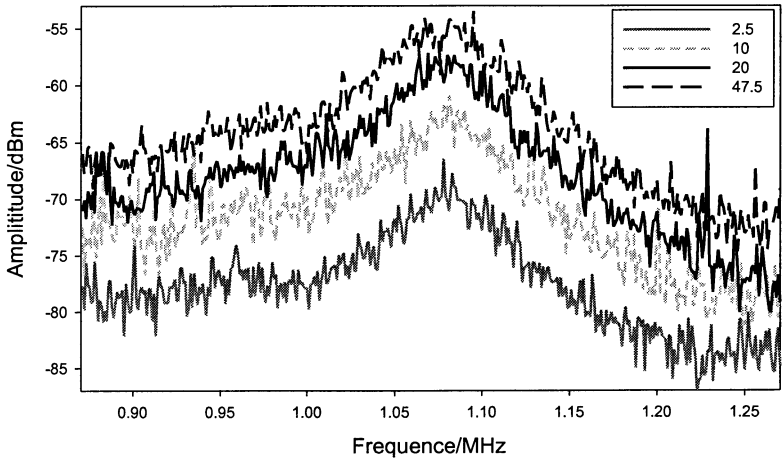

Figure 15. Spectra recorded with the focused bowl remote hydrophone at various volumetric power densities (see legend, units are W dm^{-3}) in the 'hot' spot (the liquid temperature ranged from an initial value of 22.8°C to a final value of 23.2°C). Note in these results no simultaneous DO_2 measurements could be made.

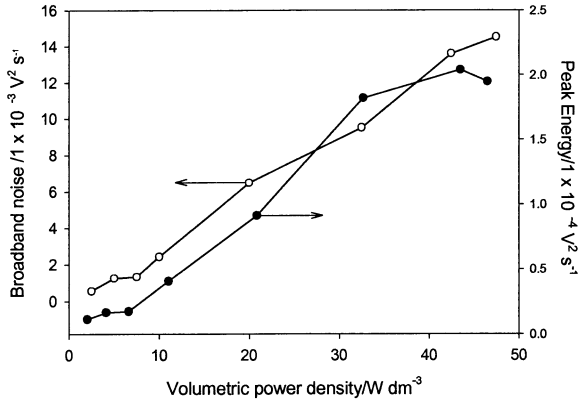

Figure 16. Data recorded with the focused bowl remote hydrophone as a function of volumetric energy density at the 'hot' spot (the liquid temperature ranged from an initial value of 22.8°C to a final value of 23.2°C). The liquid temperature ranged from an initial value of 23.2°C to a final value of 23.5°C. The 'peak' (●) energy was recorded between 1.07 to 1.09 MHz; the 'broadband' (o) energy was recorded between 0.87 and 1.27 MHz. Each data point represents a single measurement only: a national petrol strike prevented testing on the second day, in order to collect enough data for meaningful error bars.

Figure 17 shows the results of measurements taken at the 'hot' spot with the pre-prototype PCS sensor. It should be recalled that this early version lacked suitable erosion protection, and indeed cavitation damage resulting from the COMORAC tests was clearly visible on the surface of the sensor. This resulted in the comparatively poor performance shown in figure 17, compared to that obtained by later prototypes of PCS, which had more robust erosion protection. Whilst the average over three consecutive runs (inset in figure 17) increases with increasing volumetric power density (in agreement with the focussed bowl hydrophone, sonochemiluminescence and the Fricke dosimeter), variation is seen in the trends of the individual runs which make up this average (figure 17, main graph).

Figure 18 is not strictly part of the COMORAC dataset, as the measurements were taken 4 weeks after the cessation of COMORAC and used the upgraded PCS with erosion-protection. The overall sensitivity is improved over the pre-prototype COMORAC results of figure 17. The signal increases with increasing volumetric power density, agreeing with the chemiluminescent, Fricke, focussed bowl hydrophone and (as will be seen) polymer degradation data obtained in COMORAC. Furthermore, the device clearly distinguishes between the 'hot' and 'cold' spots.

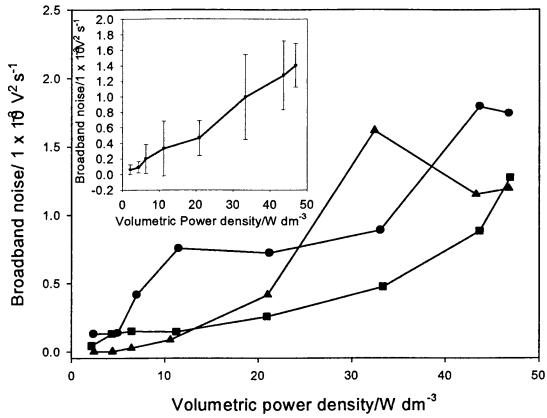

Figure 17. Data recorded with the NPL PCS 11 sensor as a function of volumetric energy density at the 'hot' spot. In these three consecutive experiments, conditions are nominally identical expect for the DO_2 and temperature readings, which were: 1.99 ppm and 21.4°C (▲); 4.13 ppm and 24.4 °C (■); and 1.86 ppm and 23.3°C (●). The insert shows the average of the data with the corresponding 90% confidence interval. Details of the spectra of the signals used to obtain these data can be found elsewhere [27, 29].

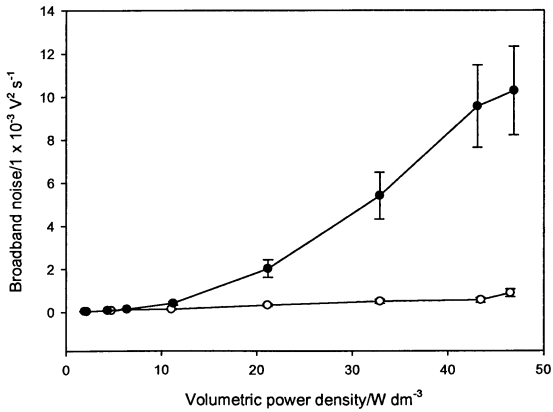

Figure 18. Plot of the broadband integrated noise from the prototype version of the PCS sensor which was produced with additional erosion protection after COMORAC. The signal is plotted as a function of volumetric power density, comparing the output from the 'hot spot' (●) to that from the 'cold' spot (○). Details of the spectra of the signals used to obtain these data can be found elsewhere [27, 29].

Of the various acoustic sensors in the IC-3 device, only the subharmonic sensing component was functional at the time of COMORAC. Since the IC-3 device uses multiple inputs to assess the level of activity, the subharmonic results on their own cannot be taken to represent the 'cavitation' level that this device would measure under normal operation. However they are presented here for two reasons. First, they give insight into the performance of the subharmonic signal *on its own* as a cavitation indicator. Second, because the full gamut of sensors in the IC-3 could not deployed, there was extra time available to explore (with the subharmonic sensor) the variation of activity within the depth of the bath.

The luminescent sensors necessarily integrate over the full depth of the water column at the hot and cold spots (with of course some biasing as a result of optical effects such as focusing and scattering). The sonochemical sensors were constrained to examine the top few centimetres of the bath: whilst in principle sample holders could be designed to operate at greater depths, the time constraints of COMORAC allowed only the sampling of the top few centimetres of the hot spot. The IC-3 however could readily be deployed to sense at various depths, and this facility was explored when it came clear that the malfunctioning of some of its modalities freed up time to do this. Figure 19 shows the results from (*a*) the top, (*b*) the middle, and (*c*) the base, of the water column under the 'hot spot'. In part (*d*) the results from the middle of the water column under the 'cold' spot are shown. Except for measurements with descending powers at the 'cold' spot, none of the results show a monotonic increase in subharmonic signal with increasing drive power density, reflecting perhaps that the subharmonic signal can be solicited from noninertial, as well as from inertial, cavitation [18§4.4.7]. This may well explain the significant hysteresis effect (and why it was not seen in figure 10): the distribution of stable bubbles in particular will be affected by whether the drive power is increasing or decreasing.

3.4 Erosion sensors

The results of the polymer degradation (dextran degradation) experiments are shown in figure 20. As expected, the molecular weight (M_n) reduces on sonication and the effect increases with applied volumetric power densities. The average number of chain breaks after 10 minutes sonication increases linearly with applied power. While the data presented cannot be used to determine the cavitation threshold in this experiment (due to the coarse nature of the power settings selected), such thresholds have previously been observed in sonochemical polymer degradation [56]. A degree of uncertainty is introduced into the results by using a natural polymer, dextran, with a wide distribution of molecular weights. Better precision could have been achieved by using a synthetic polymer with better controlled dispersity.

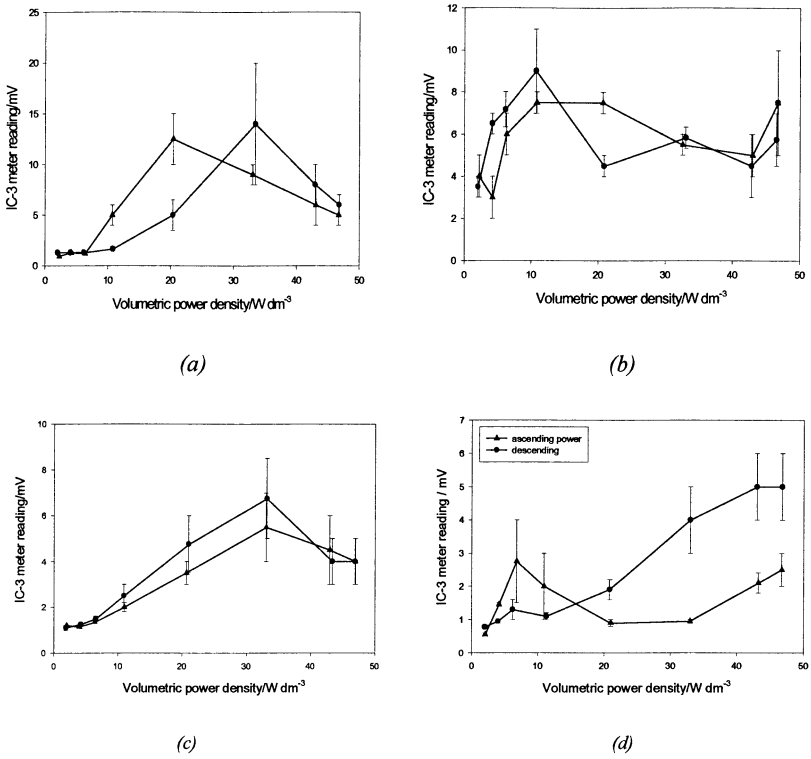

Figure 19. The output of the IC-3 meter which corresponds to the detection of the subharmonic of the tank driving frequency. Parts (*a*)-(*c*) correspond to three different vertical positions in the water column under the 'hot' spot. The symbol (▲) indicates that the data was taken with the power density increasing monotonically, and the symbol (●) indicates that it was decreasing monotonically. Part (*a*) shows results obtained 2 cm below the water surface (under the hot spot), where the initial and final temperatures (and dissolved oxygen contents) of the water were both 24.5°C and DO_2=3.0 ppm. Part (*b*) shows results obtained from the vertical centre of the bath (under the hot spot), for initial and final water temperatures of 23.2°C and 22.7°C respectively, and initial and final DO_2 readings of 1.84 ppm and 2.40 ppm respectively. Part (*c*) shows results obtained from a position 1 cm vertically above the base of the bath (under the hot spot), for initial and final water temperatures of 23.7°C and 24.1°C respectively, and initial and final DO_2 readings of 2.52 ppm and 2.81 ppm respectively. Part (*d*) shows the results obtained from the vertical centre of the tank in the 'cold' spot, where the initial and final temperatures (and dissolved oxygen contents) of the water were both 26.5°C and DO_2=4.09 ppm.

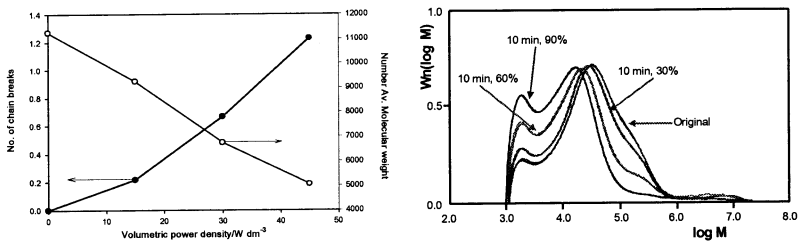

Figure 20. Plot showing the degradation of dextran (1% solution in water). Plot (*a*) shows the reduction in number average molecular weight (○) as measured by size exclusion chromatography and the average number of chain breaks (●) as a function of volumetric power density (10 minutes sonication). The chromatograms are shown in (*b*). High molecular weight chains (>10^5) are broken and the curves move to lower molecular weights. Time constraints prevented the collection of meaningful error bars.

3.5 Calorimetry

Calorimetry measures the bulk temperature rise produced by the absorption of ultrasound in the medium in the bath, as opposed to some local measure of the ultrasound at a point. It became apparent after some provisional investigations in COMORAC that, when conventional calorimetry was used (i.e. based on the average temperature rise in the whole bath – the 'bath average'), there was not going to be a measurable change in temperature at the lower power settings. For example, at a drive power density of 10 W dm^{-3}, a rise of only 0.2 °C seen over the period of measurement (5 minutes). For this reason the higher power settings only were used for 'bath average' measurements. Figure 21 shows the temperature variations during these experiments.

Regression analysis of the data shown in figure 21 enabled the volumetric power density to be estimated from calorimetry for each of the three settings measured. Table 2 shows the results of the analysis of the data. The volumetric power densities estimated by calorimetry are 20-30% of those estimated from the power input to the device (as described in section 2.1) and, although it is difficult to draw general trends from only three data points, they do not show a monotonic correlation.

Because the data of Table 2 represent averages over the whole volume of the bath, further experiments were performed in two submerged vessels (specifically a polymethylmethacrylate conical flask and a beaker). This was done to see if spatial variations could be detected and, if the temperature rises within these vessels proved to be greater than the bath average, whether this would allow measurements to be taken at the lower drive power settings.

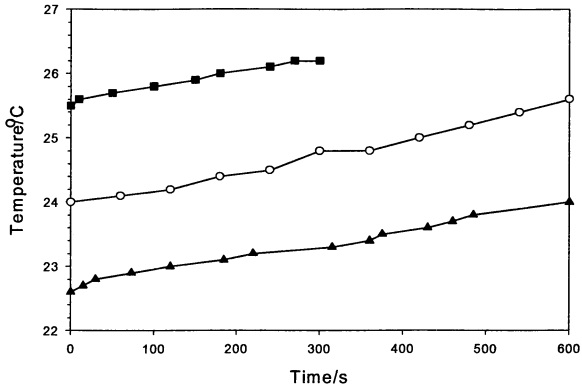

Figure 21. Plot showing the bulk temperature of the bath as a function of time for volumetric power densities 47.5 W dm^{-3} (■), 42.5 W dm^{-3} (○) and 32.5 W dm^{-3} (▲). Note the DO_2 content of the vessel varied from 2.90 ppm to 4.13 ppm during the experiment.

Table 2. Comparison of the volumetric power densities calculated from the vessel drive setting, with those estimated using calorimetry.

		Area = 23 cm x 35.8 cm = 823 cm^2	
Vessel drive setting (W dm^{-3})	*Calorimetric Power* (W)	*Calorimetric volumetric power density* (W dm^{-3})	*Calorimetric Intensity* (mW cm^{-2})
32.5	167	9.28	203
42.5	205	11.39	249
47.5	174	9.67	211

Figures 22 and 23 show the temperature profiles recorded in each case, when the vessel was placed at the cavitation 'hot' spot, as a function of the volumetric power density employed. For the corresponding drive settings, the measured temperature rises were greater than the 'bath averages' of figure 21, and measurements were therefore possible at the lower power settings. The data were fitted to polynomial curves and, from the slope of these, the power densities and the intensities of the ultrasound were estimated calorimetrically. The results are shown in Table 3.

The volumetric power densities calculated within immersed containers (e.g. the conical flask and the beaker) in Table 3 exceed those averaged over the bath (Table 2), suggesting that it is possible that these estimates reflect the presence of the 'hot' spot. However one aspect of the local heating is that the

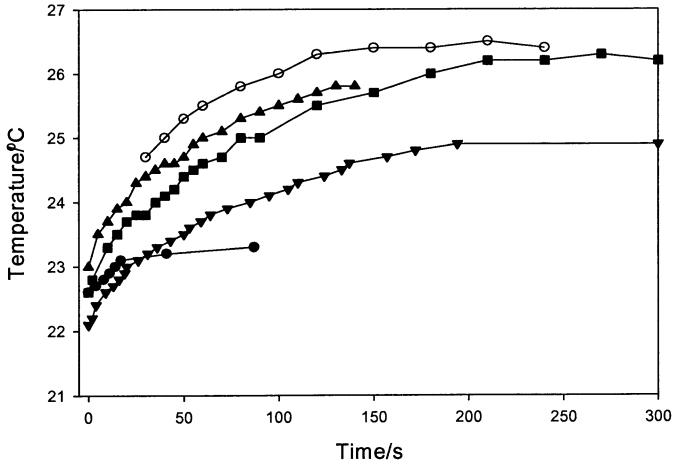

Figure 22. Plot showing the temperature profiles recorded in a conical flask placed within the test vessel. The volumetric power densities were (●) 5, (▼) 10, (■) 20, (▲) 32.5 and (○) 47.5 W dm^{-3}. DO_2 values ranged from 1.75 ppm to 2.73 ppm during the test.

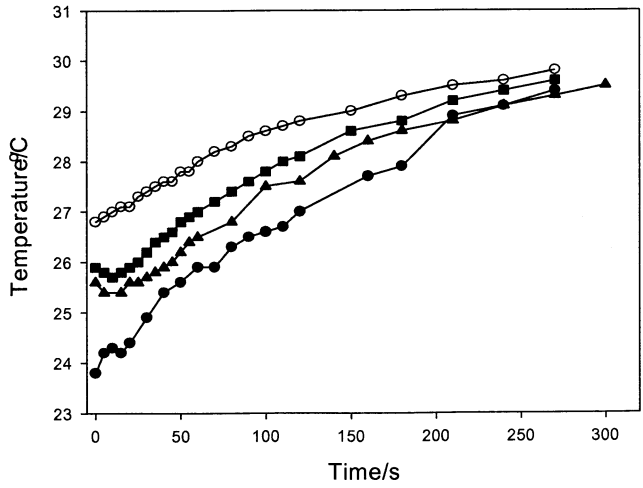

Figure 23. Plot showing the temperature profiles recorded in a beaker placed within the test vessel. The volumetric power densities were (●) 10, (▲) 20, (■), 32.5 and (○) 47.5 W dm^{-3}. DO_2 values ranged from 3.27 ppm to 4.23 ppm during the test.

Table 3. Comparison of the volumetric power density calculated from the vessel drive setting, with that estimated using calorimetry in a container within the test vessel.

Vessel setting (W dm^{-3})	Volumetric power density in conical flask (W dm^{-3})	Volumetric power density in beaker (W dm^{-3})
5	115.6	--
10	124.8	150
20	150.8	113
32.5	163.2	114
47.5	205.6	89

estimates vary with container, which will be invasive (section 2.2). The power densities estimated by calorimetry differ significantly from the nominal ones supplied by the manufacturer, which were based on the electrical input to their cleaning bath (see section 2.1). Table 2 compares 'like with like', as both sets of estimates are averaged over the bath, and here the values calculated by calorimetry are lower than those estimated from the electrical input. This might be as expected, given that both approaches seek to estimate a middle component (the sound field) by indirect means. Calorimetry uses the 'output' of the middle component, the heating, with the assumption that the heating arises when the entirety of the driving acoustic energy is converted into heat. If, as will happen, some of the driving acoustic energy is lost from the tank through other routes (transducer losses, acoustic radiation and vibration etc.), the calorimetric estimate will be an underestimate. Estimating the efficiency of the conversion of acoustic energy to heat (for calorimetry) will be a more difficult task than estimating the efficiency by which the input electrical energy is converted to the driving sound field, but errors in that estimation could in principle cause over- or under-estimates in the drive power.

4. Discussion

4.1 Comparing outputs

To compare one technique with another, each particular dataset was normalised to its own peak value. Figure 24 summarises the data from the luminescence, sonochemical, polymer degradation and acoustic sensors (normalised, and with error bars removed). Sonochemiluminescence, the Fricke reaction, polymer degradation and the focused bowl hydrophone agree well, the discrepancy between them being at worst <15 W dm^{-3} in the abscissa (figure 24(*a*)). Although quantitatively not in such good agreement with the others, the Weissler reaction nevertheless follows their general trend, but with a tendency to 'flatten out' at the highest drive powers. This characteristic is more extreme in the TA system, however, which differs qualitatively with this group, producing a significantly reduced signal at the highest drive powers (such behaviour is also seen in one of the nominally identical runs with the

pre-prototype PCS sensor in figure 17). This difference emphasises the need to understand exactly what a given device measures: Both the Fricke and terephthalic acid reactions are local measures, since both use the same confining latex test. However, TA responds to $OH^{\cdot}$ only, whilst Fricke responds to a number of radical species. Comparison of figures 13 and 14 raises the question of whether intense cavitation is depleting $OH^{\cdot}$ radicals from the solution or altering the reaction pathway in some way. In both cases a reduction in the product (2-hydroxyterephthalic acid) yield per Joule of acoustic energy would be expected. This reduction in yield at high acoustic intensities has been observed previously by von Sonntag *et al.* for an optimized TA dosimeter study in a sonochemical cell [42].

Figure 24(*b*) shows the comparison of the three acoustic detection techniques at the 'hot' spot, the only common position at which all three sensors were deployed. Note that whilst the focused bowl and IC-3 subharmonic data were taken during COMORAC, the version of the PCS sensor that was used was the one produced post-COMORAC with enhanced erosion protection. Both the focused bowl hydrophone and the post-COMORAC PCS sensor show a steady increase in the 'cavitation activity' characterised by acoustic emissions, with some indications of an activity detection threshold around the 10 W dm^{-3} level. As discussed in relation to figure 16, the broadband output from the focused bowl device in figure 22(*b*) increases with volumetric power density (in line with the Fricke and chemiluminescence techniques). Hence there is reasonable agreement between both of the broadband acoustic detection techniques of figure 23(*b*) and the chemical and optical methods shown in figure 24(*a*). Recalling that the subharmonic sensor mapped a range of behaviours (figure 19), the plot chosen for figure 24 shows a peak, achieving its maximum signal at a mid-range drive power density. Although this is qualitatively similar to the trend shown by the TA sensor, the underlying mechanism for the IC-3 signal might be associated with the generation of the subharmonic signal, not just by inertial cavitation, but also by non-inertial cavitation [18].

COMORAC was designed to test the functions of sensors within imposed time constraints and, with the exception of the PCS sensor, in an unfamiliar laboratory. With these time constraints, the limited precisions and random errors associated with measurements did not provide an environment in which to investigate the existence of suggestive trends. COMORAC was not designed to determine the trends of each technique, nor the associated errors, precisely: this would require a different type of experiment (the type more usually reported in the literature), where a great deal of time is spent refining a single technique and reducing the inherent uncertainties. Therefore any trend in the COMORAC data can only be viewed as suggestive, particularly when time constraints allowed only preliminary estimations of the uncertainties. Suffice to say that these preliminary results suggest that the systems group themselves

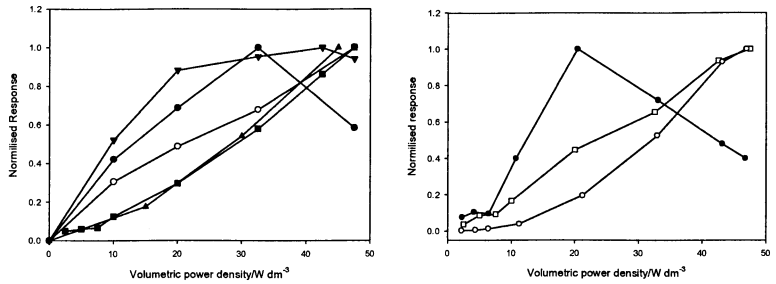

Figure 24. Summary of normalized results (error bars removed) against volumetric power density. (*a*) The sonochemical results for the TA (●), Fricke (○), and Weissler reactions (▼), sonochemiluminescence (■), (▲) polymer degradation. (*b*) Two of the acoustic sensors used in COMORAC (the IC-3 subharmonic (●) and the broadband output of the focused bowl hydrophone (□)), plus data taken 4 weeks after COMORAC with the upgraded PCS system used for the data of figure 18 (○). From of the range of datasets taken to represent the IC-3 in this comparison, the set associated with increasing power from figure 19(*a*) (*i.e.* taken just below the surface of the water) were used. This is because these conditions agree most closely with those under which the sonochemical datasets were taken.

into two sets. In the first group (denoted as Group α) the output of the sensing system generally increases with rising volumetric power density. This group includes the focussed bowl hydrophone (for broadband signal), the Fricke dosimeter, the polymer degradation, the sonochemiluminescence, and the post-COMORAC version of the PCS (figure 24). Figure 25 shows the normalised response for Group α systems. In the second group (denoted as Group β) a varied response with volumetric power density has been observed. This group includes the IC-3, the Weissler, the TA dosimeter (figure 24(*a*)), and some of the results obtained with the pre-prototype version of the PCS used in COMORAC (figure 17). Without error bars it is difficult to assign significance to trend shown by the peak signal of the focused bowl (figure 16).

To ask which grouping exhibits the 'true' trend is not the correct question. Both trends are 'reasonable', in that whilst cavitational activity might in general be expected to increase with increasing drive power, this trend cannot continue indefinitely (because of a range of effects including shielding, degassing, heating, nonlinearities in the driver or sensors [19]). Given their different mechanisms and sampling characteristics, it would not be surprising to find that certain sensors 'flatten out', or even show a reduced signal, at the highest drive power densities (once such effects have been confirmed to be significant within the associated errors). The actual question must be based on

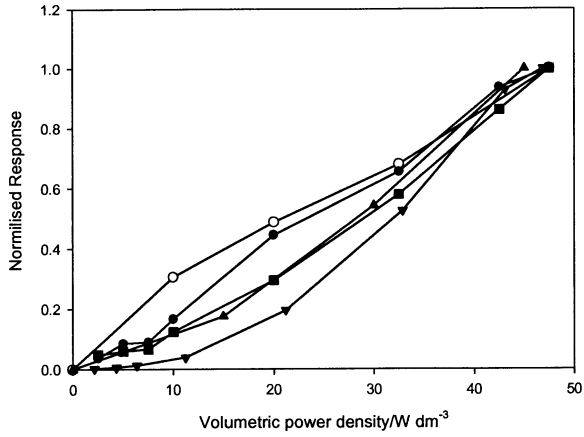

Figure 25. Plot showing the sensor systems that give a broadly similar response (Group α) with respect to volumetric power density. Broadband signal from focussed bowl hydrophone (●), Fricke reaction (○), post-COMORAC PCS sensor (▼), sonochemiluminescence (■) and (▲) polymer degradation.

knowledge of what effect it is of prime importance to measure in a given circumstance (e.g. soil cleaning, erosion, bioeffect). We shall call this the 'primary effect'. The question is then which of the sensors follow the same measurement trend as the primary effect (taking into account both sampling and associated errors). That sensor then becomes important if its use to measure cavitational activity offers advantages (in terms of invasiveness, speed, requirement for specialist expertise and facilities etc.) over measuring the primary effect directly.

4.2 Performance comments on individual techniques

The following subsections give the opinion of the researchers in using the various techniques. It should be recalled that these are not necessarily comments on the technique *per se*, but on how they performed under the constraints of time and geography in measuring a cavitation field in an unfamiliar laboratory, imposed by the COMORAC regime.

4.2.1 Luminescences

The chemiluminescent imaging technique has been crucial in providing a practical and rapid way of differentiating between 'hot' and 'cold' spots in cavitation activity. It is a powerful means of establishing inhomogeneities, even in three dimensions [6]. It probably remains the only practical means

which might be applied for this purpose, if time-intensive scanning and mapping of the volume is not workable. Of course many of the local sensors could be attached to a scanning rig, but the operation would be laborious and lack the ability to measure all points simultaneously. In addition, most of these sensors require a physical body to be inserted into the liquid, with the commensurate implications for invasiveness described in section 2.2. If the signal level is sufficiently strong, luminescence may be used to image in real time the effect on the cavitation field of the insertion of another sensor. In photon counting (or equivalent) mode, chemiluminescence gives rapid quantification, and the apparatus is remote. It cannot however be said to be non-invasive: The disadvantages of chemiluminescence is that it requires specialised chemicals (e.g. strong alkali) and requires blackout. Perhaps a more subtle characteristic is that, when used as a remote sensor in the manner applied in COMORAC, the footprint depends on the levels of signal and noise, since its edges are defined relative to when the detected level of luminescence is indistinguishable from the noise. Confining the sensing volume by opaque material can ameliorate this, but of course involves insertion of a solid into the cavitating field, with the commensurate questions regarding invasiveness.

Multibubble sonoluminescence provided a weaker signal than chemiluminescence, and hence the requirement for blackout is even stricter. A low signal-to-noise ratio (SNR) may limit its usefulness, but if this can be overcome (with sufficient blackout, cooled photomultipliers [57] etc.) it has several advantages. In principle sonoluminescence could be used to map out the cavitation field, but SNR was generally too low to do this. If the SNR is sufficient, sonoluminescence can rapidly produce a quantitative output. Unlike sonochemiluminescence, it does not require specialised chemicals and this, with its remote equipment, makes it non-invasive. In principle therefore it should have been the only sensor that was sufficiently non-invasive to be used simultaneously with all other sensors, in order to provide a baseline monitor for the stability of the performance of the bath. However the data so obtained had high uncertainties because of the low SNR. As with sonochemiluminescence, the extent of the footprint for remote sensing is governed by the levels of signal and noise, and this is likely to be an even more important consideration during calibration for sonoluminescence because the SNR is generally lower. Again, the use of optically opaque walls to confine the sample volumes can enhance the definition of the footprint and sampling volume [30,31], but require a physical presence to invade the sample which can be invasive even if that presence is acoustically transparent (see section 2.2).

Disadvantages which are common to both chemiluminescence and sonoluminescence detectors are the following requirements:

- blackout;
- specialist and relatively expensive high gain equipment;
- appreciation of the effects of signals and noise, which in turn require staff training;
- an understanding of the various spurious light sources (light can scatter from structures in unexpected ways; and faint moisture-induced sparks can generate light emissions in the pulsing sequence expected for the light emission).

4.2.2 Sonochemical sensors

The sonochemical sensors have numerous similarities. All worked well, although it is recognised that the researchers in this case had significant expertise. The tests were physically invasive (in that a test sample holder was immersed in the cavitation field), required the introduction of specialised chemicals, and in this experiment some were not real-time (because of the need to remove samples for spectrophotometry). However, the introduction of electrochemical measures in this experiment provided a route for continuous sonochemical monitoring that is close to real-time [39]. This could however only be deployed for the Fricke and Weissler reactions, and is not suitable for the TA sensor, which alone has no electrochemical alternative to fluorescence. However all three chemical dosimeters (TA, Fricke and Weissler) could be used with a similar continuous flow method that exploits spectroscopic detection, although this would add significant complication and cost to the method. Sampling, as used in COMORAC, allows relatively "low-tech" apparatus (akin to colourimeters used for water analysis or some medical diagnoses) to be deployed. This mitigates the requirement for specialist equipment and staff.

Whilst the Fricke reaction has an increasing signal for increasing drive power density, the Weissler reaction showed indications of 'flattening out' at the highest powers, and the TA sensor gave a reduced signal at the highest drive powers. The reasons for these possibly lie in the nature of the different reactions involved (section 4.1). The Fricke reaction has the unique advantage in that it has a well-characterised dosimetry for ionising radiation.

4.2.3 Acoustic sensors

The focussed bowl showed a gradual increase in the cavitation activity up to the maximum power density of the test. Given its general conformance within the Group α trend, this is an unexpectedly promising result, since the sensor in question was designed for the detection of cavitation from micro-second duration pulses, and not transient cleaning bath fields.

The PCS sensor, which ostensibly detects a similar signal to the focused bowl device, suffered greater exposures to ultrasound than any other sensor, and COMORAC consequently identified within it a susceptibility to erosion

damage from prolonged use. Whilst this damage caused the device to underperform in COMORAC (as evidenced for example by the poor repeatability in figure 17), the upgrade undertaken as a consequence of COMORAC produced a device which, 4 weeks after COMORAC, followed the Group α trend, and has sufficient spatial resolution to distinguish between the 'hot' and 'cold' spots (figure 18). The design modifications after COMORAC increased the resistance of the sensor to cavitation erosion by the insertion of a thin protective player covering the electrode, along with significant improvements in the method of forming the electrical contact.

Whilst the upgraded PCS sensors has yet to be tested in a full COMORAC-like trial, it has been used successfully in a number of studies by NPL and outside organisations [27, 29, 43-47], and the output of the device has been shown to correlate well with erosion studies carried out using thin foils of aluminium [55]. Although the PCS has been designed to minimise the perturbation due to the direct acoustic field, it is clearly an invasive sensor with regards the liquid body (see section 2.2). Nevertheless, it may provide an appropriate tool for assessing cavitation activity for application at industrial level, as it requires no special operating conditions and can be used in aqueous media.

Whilst the PCS was subjected to the most erosive conditions during COMORAC out of the various sensors used, the IC-3 sensor was subjected to the most arduous journey to reach NPL for testing in COMORAC. Because of the resulting damage, only the subharmonic sensor worked. It detected strong subharmonic at low driving powers, and subharmonic emission by non-inertial cavitation would be the most likely cause of this. Because of this, the sensor normally operates by measuring both subharmonic and broadband signals. It was the latter facility that suffered damage when the device was in transit to the UK from Belarus for the COMORAC tests, and no broadband data could be measured with it. Hence, COMORAC cannot be seen as a true measure of the optimal performance of this device.

4.2.4 Erosion sensors

With the exception of polymer degradation (which could arguably be classed as a sonochemical rather than a erosion sensor), the erosion-based sensors failed to yield a result in the strict timescale limits of the COMORAC experiment. In all cases this was not because of the technique *per se*, but because of the limitations of the restricted and set time scale. The particle erosion and foil erosion sensors were added to COMORAC opportunistically and with little prior preparation. In the case of particle erosion, this was done in the spirit of conducting a look-see study, but in the case of foil erosion it was because the received wisdom regarding the simplicity of its use is misleading.

The erosion of aluminium foil has often been cited as a possible standard (section 1.2), though this is probably because of its cheapness and the perception that it is easy to use. Despite this, the foil erosion method has in the past proved to be impossible to standardise. In the COMORAC tests, the foil was mounted in a frame, and the area of pinhole generation was integrated for each test by monitoring the light transmission through the foil. However whilst foil testing lived up to its reputation as being perhaps the simplest from which to obtain a result, there was so little consistency in those results that they did not warrant publication. Certain features are clear: the degree and distribution of the pinholes was overwhelmingly dominated by the mounting (rigid frames attracting cavitation, for example). The foil itself was invasive and, with the frame, influenced the nature of the cavitation. Pinhole generation is the result of a particular form of cavitation, which may be an advantage (if that erosion correlates to the purpose for which the measurement is being made) or disadvantageous (if it does not). It is telling that, despite it being supported by many over 4 decades as the preferred technique for a providing a standard, foil erosion has never been successfully realised as such. The over-riding disadvantage of this technique for the researchers who tried it in COMORAC was the reputation it has of being simple to use: because of this, insufficient preparatory time was spent prior to COMORAC to make it useable. Subsequent to the experience of COMORAC, time was spent in laying down sufficient expertise in the foil erosion test [55]. It has not yet been tested under COMORAC-like conditions.

Another erosive measure, electrochemical erosion monitoring, is in principle responsive to erosive events in general, is real time, each element in a sensor has a defined sensing area of typical diameter 25-125 μm giving high spatial resolution [53,54], and high sensitivity. At the time of the COMORAC test it was a very new technology, and insufficiently robust to generate publishable results in the timeframe allowed by COMORAC. Since COMORAC the technique has been developed and performs well in controlled conditions [52-54], although it has yet to be subjected to another COMORAC-type study.

4.2.5 Calorimetry

Calorimetry is in a class of its own, in that it does not measure cavitation but rather the heating of the sample. Of course none of the techniques in COMORAC measure 'cavitation', if such a phrase has meaning, but rather the effects of cavitation (be they sonochemical, erosive, luminescent or acoustic). However these effects are dominated by cavitation, and often can only be produced by it. Heating of a sample subjected to power ultrasound can come about through a variety of mechanisms, including cavitation, conductive heating from transducers, and direct heating of the (bubbly) liquid by

absorption of the acoustic power [58]. The propensity to generate the calorimetry signal through non-cavitational mechanisms by no means negates its usefulness, but is a feature which must be understood when it is applied: calorimetry does not measure cavitation. Normal practice is to convert the measured temperature rise into an equivalent 'acoustic power', a conversion which requires certain assumptions (section 2.2.2(*d*)).

Similarly, whilst some techniques are invasive in terms that a physical entity must be inserted into the cavitation cloud, some are invasive in that by-products of the activity being measured change the cavitation environment (such as particles generated by erosion in a foil sensor seeding new cavitation event). Again calorimetry is special in this respect, in that the cavitation environment is changed, not as a result of a by-product of the measurement, but by the very signal being measured. For calorimetry to generate a signal, the liquid temperature must change, the commensurate change in sound speed can dramatically change the cavitation if the sound field is strongly modal [6] (figure 2). There is of course a history of published data indicating changes in cavitational effects (such as multibubble sonoluminescence) with liquid temperature [18§5.2.2(*b*)(*iii*)], although no doubt the mechanism by which this occurs can vary with the experimental conditions. For example, the ambient temperature not only affects the dynamics of single bubbles, but also the behaviour of the population through, for example, gas solubility. Whilst therefore calorimetry by definition measures a changing environment, the subsequent effects are minimised if the temperature plots obtained in the exercise are extrapolated back to time zero when heating first occurred.

Conventional calorimetry uses estimates of the spatially averaged temperature rise in the bath (the 'bath-average') to estimate the acoustic power input. Because the large volume of the bath in COMORAC meant that the rates of temperature rise were not large, measurable temperature rises were only detectable for the higher drive power settings. Only the bath-average calorimetric estimates can be compared with the input power densities estimated from the electric input to the transducers, since the latter are also 'bath-averages'. The volumetric power densities estimated using calorimetry were 20-30% those estimated from the driver settings. Use of inserted vessels in an attempt to localise the measure generated higher calorimetric averages, although no attempts were made to minimise the invasiveness of the inserted vessel.

In summary, calorimetry is simple to use, but the signal can arise from non-cavitation effects and a temperature rise can prove to be invasive. Additionally, the conversion of the measured temperature rise to 'acoustic

power' assumes that all acoustic energy is converted to heat; and assumes a certain radiating area; and assumes no direct heating from transducers.

5. Conclusions

The bulk of our experience with multibubble cavitation comes from partially understood observations in poorly characterised acoustic cavitation fields. We do not measure 'cavitation' itself: indeed we have trouble defining what the term means. For decades possible standard or commercial methods of 'measuring' cavitation have been proposed. Each measures some effect produced by cavitation and, sometimes, by non-cavitational effects. To obtain a useful measure for 'cavitation', we must first identify the cavitation-mediated effect which we wish to monitor (the 'primary effect'). Then we must find that effect which not only mimics the primary effect in its generation, but which also is in some way more practicable to measure than is direct measurement of the primary effect.

COMORAC examined a selection of possible techniques, though not an exhaustive list (there were for example no biological sensors). The over-riding feature of COMORAC addressed the fact that the published performance of candidate techniques in the past has been dominated by results obtained in close-to ideal conditions, with expert users (often the inventors or advocates of the technique), familiar laboratories and a generous timescale in which to produce the best results. However for a technique to be adopted as a practical cavitation sensor by industrial users, none of these luxuries can be a pre-requisite for adequate performance. Hence COMORAC took place in a laboratory and cavitating sample which was unfamiliar to all except the NPL users, and researchers were given a set 2-day period in which to complete the full range of candidate techniques they wished to deploy. Not all techniques were tested on a 'level playing field': particle erosion, for example, was introduced on a look-see basis, and was just one of many techniques which the University of Bath wished to try in their two-day period. Hence when early difficulties were encountered it had to be abandoned to make way for other techniques from Bath. Clearly this technique had less chance of succeeding than would a sensor that was the sole candidate proposed by a researcher in their two-day period.

The restrictions in time and location imposed by COMORAC made the conditions for taking measurements more difficult than are often encountered in published accounts of cavitation detection. Whilst it would be possible to redesign COMORAC to facilitate more detailed experimentation, this may dilute the inherent and unique nature of the test. If equal time were made available for each test, as opposed to each researcher, this would preserve the spirit of COMORAC and provide a more 'level playing field' for comparing techniques and enable proper testing of, for example, 'hot' and 'cold' spots.

However several of the experimenters complained that the time expended on each individual experiment was too short to enable real confidence in the results to be obtained, noting that in some cases the experiments were only run once due to time restrictions. Whilst it would be preferable to have included more data on repeatability, to allow too long would detract from the inherent message of COMORAC, which is a test of how useful the technique might be in the time-constrained conditions of industrial use. Similarly there were suggestions that it would be better to move the cavitating sample around the country to the various investigators, and leave it for an extended period to enable repeat testing. This would be a sensible experiment, but it would denude COMORAC of its key feature to require a technique to perform 'on cue', may cause delays, and reduces the chance of there being consistent operation of the reference bath and medium by allowing the presence of the same dedicated staff at each test. It is likely that later COMORAC tests may prove to be 'variations on the theme' of this first test (which emphasised the need to perform on cue), such that successive tests could stress different aspects, such as repeatability and long term stability.

The difficult conditions imposed by COMORAC on the experimenters resulted in the redesign and enhancement of several of the techniques (the PCS system, the electrochemical erosion monitor, and the foil system). In addition they allowed criticism of the reference cavitating sample (i.e. the reference tank and liquid), which is considered to be a work-in-progress and is currently undergoing redesign. COMORAC identified some potential improvements, including enhanced temperature and gas control, and the ability to pressurise to enhance or suppress cavitation. Some features of the bath, whilst they hampered the experimenters in COMORAC (e.g. the existence of metallic walls causing electrical noise problems with the electrochemical equipment employed, the large volume being inappropriate for complete sonochemical monitoring and making calorimetry insensitive), would likely be characteristic of a commercial cleaning baths as discussed in section 2.2.

The importance of the early appreciation in COMORAC of the inhomogeneity of the cavitation field cannot be underestimated. If, when undertaking a measurement, an *a priori* assumption is made that the cavitation activity is homogeneous, any test which is reliant on local cavitation activity will produce equivocal results, since one local measurement cannot be extrapolated to the volume as a whole. In COMORAC all of the sensors, except the imaging of sonochemiluminescence, were local tests. A local sensor can be scanned through the cavitation field to map it. This is time-consuming, but valid within the constraints placed on the measurement by the stability of the cavitation field and the invasiveness of the sensor. The most important point is that no assumption of field homogeneity must be made if the sensor is local. The technique which addressed the inhomogeneity of the cavitation field

most conveniently was the imaging of sonochemiluminescence. This provided a rapid way of assessing the inhomogeneity of the cavitation activity, and can readily be extended to three dimensions [6]. If the equipment and expertise is available, this is an extremely valuable procedure: using video, it can in real time follow the distribution of cavitation activity real-time as, for example, the drive power, liquid temperature (and consequently mode structure) etc. change, or as other sensors are introduced (to assess their invasiveness). However the evaluation of such luminescence measurements must be tempered by the fact that, although in COMORAC they were indispensable, they also proved to be the techniques which required most expertise and specialist equipment to set up. Perhaps the most universal finding of COMORAC is that there is no simple answer to cavitation monitoring.

To conclude, in many ways the above concerns reflect the fact that it could be said that COMORAC was in a way premature: the 'ideal' sensor had not been found to characterise the bath before the test, and such a characterisation would have removed some of the uncertainties in testing. For example, the results of figure 19 suggest that in fact the inhomogeneity in all three dimensions should be examined, and fuller characterisation of the vessel prior to COMORAC would assist this. Similarly, some sensors showed hysteresis to such an extent that averaging the results obtained when the drive power was increasing, with those obtained when it was decreasing, would have masked important features and been statistically dubious (the error bars of the two curves do not for example overlap in key parts of figure 19). Other sensors could not detect such a large degree of hysteresis (figure 10 and section 2.1), perhaps reflecting the differing methods of generation of the signal. However to propose that COMORAC should have had these improvements is to suggest that there is a 'correct' answer to inhomogeneity, hysteresis, and the other issues raised in this section. This in turn presupposes that the 'ideal' technique has already been found. Yet it cannot be identified without COMORAC testing. This 'Catch-22' situation can only be resolved by proposing a series of COMORAC tests, where the sensors, medium and vessel are iteratively improved using the knowledge of preceding COMORAC tests (see section 1.3). Indeed, subsequent to this first COMORAC test, the test vessel and several sensors have been improved upon, in preparation for the next COMORAC experiment.

Acknowledgments

The authors acknowledge the financial support of the National Measurement System Directorate of the UK Department for Trade and Industry. These data and conclusions were first presented to the Joint 140th Meeting of the Acoustical Society of America/NOISE-CON 2000 (Newport Beach, USA, 2000) [59].

References

1. T. G. Leighton, "From seas to surgeries, from babbling brooks to baby scans: The acoustics of gas bubbles in liquids," *International Journal of Modern Physics B,* **18**(25), 3267-3314 (2004).
2. T. G. Leighton, "A strategy for the development and standardisation of measurement methods for high power/cavitating ultrasonic fields: Review of cavitation monitoring techniques," *ISVR Technical Report No. 263, University of Southampton* (1997).
3. B. Zeqiri, M. Hodnett and T. G. Leighton, "A strategy for the development and standardisation of measurement methods for high power/cavitating ultrasonic fields – Final project report," *NPL Report CIRA(EXT)016 for National Measurement System Policy Unit (Department of Trade and Industry)* (1997).
4. P. N. Gélat, M. Hodnett and B. Zeqiri, "Establishing a reference ultrasonic cleaning vessel: Part 1: Supporting infrastructure and early measurements," *NPL Report CMAM* (Centre for Mechanical and Acoustical Metrology) 55 (2000).
5. M. Hodnett, B. Zeqiri, N. Lee, P. N. Gélat, "Report on the feasibility of establishing a reference cavitating medium - final project report," *NPL Report CMAM* (Centre for Mechanical and Acoustical Metrology) *58* (2001).
6. P. R. Birkin, T. G. Leighton, J. F. Power, M. D. Simpson, A. M. L. Vincotte and P. F. Joseph, "Experimental and theoretical characterisation of sonochemical cells. Part 1: Cylindrical reactors and their use to calculate speed of sound," *J. Phys. Chem. A,* **107**, 306-320 (2003).
7. R. A. Roy, S. Madanshetty and R. E. Apfel, "An acoustic backscattering technique for the detection of transient cavitation produced by microsecond pulses of ultrasound," *J. Acoust. Soc. Am.,* **87**, 2451-2455 (1990).
8. C. K. Holland, R. A. Roy, R. E. Apfel and L. A. Crum, "*In-vitro* detection of cavitation induced by a diagnostic ultrasound system," *IEEE Trans on UFFC,* **39**, 95-101 (1992).
9. S. I. Madanshetty, R. A. Roy and R. E. Apfel, "Acoustic microcavitation: its active and passive detection," *J. Acoust. Soc. Am.*, **90**, 1515-152 (1991).
10. A. J. Coleman, M. J. Choi, J. E. Saunders and T. G. Leighton, "Acoustic emission and sonoluminescence due to cavitation at the beam focus of an electrohydraulic shock wave lithotripter," *Ultrasound in Medicine and Biology*, **18**, 267-281 (1992).
11. A. J. Coleman, M. Whitlock, T. G. Leighton and J. E. Saunders, "The spatial distribution of cavitation induced acoustic emission, sonoluminescence and cell lysis in the field of a shock wave lithotripter," *Phys. Med. Biol.,* **38**, 1545-1560 (1993).
12. A. A. Atchley, L. A. Frizzell, R. E. Apfel, C. K. Holland, S. Madanshetty and R. A. Roy, "Thresholds for cavitation produced in water by pulsed ultrasound," *Ultrasonics*, **26**, 280-285 (1988).
13. C. K. Holland and R. E. Apfel, "Thresholds for transient cavitation produced by pulsed ultrasound in a controlled nuclei environment," *J. Acoust. Soc. Am.*, **88**, 2059-2069 (1990).
14. "Cavitation activity measuring procedure", *Report from the Ultrasonic Manufacturers Association Inc.*, (1964).
15. "Ultrasonic cleaning equipment standard," *Report from the Ultrasonic Manufacturers Association Inc.*, (1964).

16. A. E. Crawford, "The measurement of cavitation," *Ultrasonics*, **2**, 120-123 (1964).
17. A. Weissler, "A chemical method for measuring relative amounts of cavitation in an ultrasonic cleaner," *Institute of Radio Engineers (IRE) International Convention Record*, part 6, pp. 24-30 (1962).
18. T. G. Leighton, *The Acoustic Bubble* (Academic Press, London) (1994).
19. T. G. Leighton, "Bubble population phenomena in acoustic cavitation," *Ultrasonics Sonochemistry*, **2**, S123-136 (1995).
20. R. M. G. Boucher and J. Kreuter, "Measurement of cavitation activity in ultrasonic cleaners.," *Contamination Control*, pp. 16-18 (March 1967).
21. R. M. G. Boucher and J. Kreuter, "The measurement of cavitation activity in ultrasonic cleaners," *Macrosonics Corporation, Internal Report* (1966).
22. A. Weissler, "Ultrasonic cavitation measurements by chemical methods," *Fourth International Congress on Acoustics* (Copenhagen), **J.32**, pp. 21-29 (1961).
23. S. Basu, "Accelerated cavitation screening of organic coatings using acoustic emission technique," *Trans. ASME, J. of Vibration, Stress, and Reliability of Design*, **106**, 560-564 (1984).
24. Note that attempts have been made to formalise the distinction between driver and cavitation-related noise in erosive devices – see M. E. Schafer and A. Broadwin, "Acoustical characterization of ultrasonic surgical devices," *Ultrasonics Symposium*, pp. 1903-1906 (1994).
25. "Specification for sonic cleaning equipment," Writing Group S1-W-31, American Standards Association (1963).
26. P. R. Birkin, J. F. Power, A. M. L. Vinçotte and T. G. Leighton, "A 1 kHz frequency resolution study of a variety of Sonochemical Processes," *Physical Chemistry Chemical Physics*, **5**, 4170-4174 (2003).
27. B. Zeqiri, N. D Lee, M. Hodnett and P. N. Gélat, "A novel sensor for monitoring acoustic cavitation. Part II: Prototype performance evaluation," *IEEE Transactions on Ultrasonics, Ferroelectrics and Frequency Control*, **50**, 1351-1362 (2003).
28. P. R. Birkin, D. G. Offin, P. F. Joseph and T. G. Leighton, "Cavitation, shock waves and the invasive nature of sonoelectrochemistry", Journal of Physical Chemistry **B 109**(35), 16997-17005 (2005).
29. B. Zeqiri, P. N. Gélat, M. Hodnett and N. D. Lee, "A novel sensor for monitoring acoustic cavitation. Part I: Concept, theory and prototype development," *IEEE Transactions on Ultrasonics, Ferroelectrics and Frequency control*, **50**, 1342-1350 (2003).
30. T. G. Leighton, M. J. W. Pickworth, A. J. Walton and P. P. Dendy, "Studies of the cavitational effects of clinical ultrasound by sonoluminescence: 1. Correlation of sonoluminescence with the standing-wave pattern in an acoustic field produced by a therapeutic unit," *Physics in Medicine and Biology*, **33** (11), 1239-1248 (1988).
31. G. W. Ferrell and L. A. Crum, "A novel cavitation probe design and some preliminary measurements of its application to megasonic cleaning," *J. Acoust. Soc. Am.*, **112**, 1196-1201 (2002).
32. M. Bertholet, "Sur quelques phénomènes de dilation forcée des liquids," *Annales de chimie et de physique Series 3*, **30**, 232-237 (1850).
33. J. L. Green, D. J. Durben, G. H. Wolf and C. A. Angell, "Water and solutions at negative pressure: Raman spectroscopic study to -80 Megapascals," *Science*, **249**, 649-652 (1990).

34. R. Chow, R. Blindt, R. Chivers and M. Povey, "The sonocrystallisation of ice in sucrose solutions: primary and secondary nucleation," *Ultrasonics*, **41**, 595-604 (2003).
35. L. McCausland and P. Cains, "Ultrasound to make crystals," *Chemistry & Industry* **5**, 15-17 (2003).
36. R. D. Dennehy, "Particle engineering using power ultrasound," *Organic Process Research and Development*, **7**, 1002–1006 (2003).
37. H. N. McMurray and B. P. Wilson, "Mechanistic and spatial study of ultrasonically induced luminol chemiluminescence," *Journal of Physical Chemistry A*, **103**, 3955-3962 (1999).
38. C. von Sonntag, G. Mark, A. Tauber and H.P. Schuchmann, "OH radical formation and dosimetry in the sonolysis of aqueous solutions," In: *Advances in Sonochemistry* (JAI Press) Vol. 5, pp. 109-145 (1999).
39. P. R. Birkin, J. F. Power, T. G. Leighton and A. M. L. Vinçotte, "Cathodic Electrochemical Detection of Sonochemical Radical Products," *Analytical Chemistry*, **74**, 2584-2590 (2002).
40. G. J. Price and E. J. Lenz, "The use of dosimeters to measure radical production in aqueous sonochemical systems," *Ultrasonics*, **31**, 451-455 (1993).
41. H. Fricke and E. J. Hart, *Radiation Dosimetry*, 2nd Edition, Volume II - Instrumentation, (Ed. F. H. Attix and W. C. Roesch, Academic Press, New York) 167-239, (1966).
42. G. Mark, A. Tauber, R.Laupert, H. P. Schuchmann, D. Schulz, A. Mues and C. v. Sonntag, "OH-radical formation by ultrasound in aqueous solution – Part II: Terephthalate and Fricke dosimetry and the influence of various conditions on sonolytic yield," *Ultrasonics Sonochemistry*, **5**, 41-52 (1998).
43. F. Fedele, A. J. Coleman, T. G. Leighton, P. R. White and A. M. Hurrell, "Development of a new diagnostic sensor for Extra-corporeal Shock-Wave Lithotripsy," *Proceedings of the First Conference in Advanced Metrology for Ultrasound in Medicine*, *Journal of Physics: Conference Series* **1**, 134-139 (2004).
44. M. Hodnett, R. Chow and B. Zeqiri, "High-frequency acoustic emissions generated by a 20 kHz sonochemical horn processor detected using a novel broadband acoustic sensor: a preliminary study", *Ultrasonics Sonochemistry*, **11**, 447-454 (2004).
45. F. Fedele, A. J. Coleman and T. G. Leighton, "Use of a cylindrical PVdF hydrophone in a study of cavitation adjacent to stone phantoms during extracorporeal shockwave lithotripsy," *Proc of the 9th Annual National Conference of the Institute of Physics and Engineering in Medicine*, (IPEM, Bath) p. 66 (2003).
46. F. Fedele, A. J. Coleman, T. G. Leighton, P. R. White and A. M. Hurrell, "A new diagnostic sensor for Extra-corporeal Shock-Wave Lithotripsy," *Acoustics Bulletin* **29**, 34-39 (2004).
47. F. Fedele, A. J. Coleman, T. G. Leighton, P. R. White and A. M. Hurrell, "Development of a new diagnostic device for Extracorporeal Shock-Wave Lithotripsy," *Proceedings of the X Mediterranean Conference on Medical and Biological Engineering "Health in the Information Society"* (31 July-5 August 2004), IFMBE Proceedings Volume 6, 2004; CD proceedings paper no. 54 (4 pages) (2004).
48. K. S. Suslick, G. Price, "Applications of Ultrasound to Materials Chemistry", *Annu. Rev. Matl. Sci.*, **29**, 295-326 (1999).
49. G. J. Price, A. W. White and A. A. Clifton, "The effect of high intensity ultrasound on solid polymers", *Polymer*, **36**, 4919-4926 (1995).

50. G. J. Price, F. Keen and A. A. Clifton, "Sonochemically assisted modification of polyethylene surfaces" *Macromolecules*, **29**, 5664-5670 (1996).
51. T. Prozorov, R. Prozorov, K. S. Suslick, "High Velocity Inter-Particle Collisions Driven by Ultrasound", *J. Am. Chem. Soc.*, **126**, 13890-13891 (2004).
52. P. R. Birkin, R. O'Connor, C. Rapple and S. Silva-Martinez, "Electrochemical measurement of erosion from individual cavitation generated from continuous ultrasound," *Journal of the Chemical Society Faraday Transactions*, **94**, 3365-3371 (1998).
53. P. R. Birkin, D. G. Offin and T. G. Leighton, "Experimental and theoretical characterisation of sonochemical cells - Part 2 Cell disruptors (Ultrasonic horns) and cavity cluster collapse," *Physical Chemistry Chemical Physics*, **7**, 2005, 530 - 537.
54. P. R. Birkin, D. G. Offin and T. G. Leighton, "The study of surface processes under electrochemical control in the presence of inertial cavitation," *Wear*, **258**/1-4, 623-628 (2004).
55. B. Zeqiri, M. Hodnett and A. J. Carroll, "Studies of a novel sensor for assessing the spatial distribution of cavitation activity within ultrasonic cleaning vessels", *Ultrasonics* (in press) (2005).
56. G. J. Price, *Polymer Sonochemistry: Controlling the Structure of Macromolecules.* In "Sonochemistry and Sonoluminescence" L.A. Crum, T.J. Mason, J. L. Reisse and K.S. Suslick (Eds) NATO ASI Series 524 Kluwer, Dordecht, pp. 321-344 (1998).
57. T. G. Leighton, M. J. W. Pickworth, J. Tudor and P. P. Dendy, "Studies of the cavitational effects of clinical ultrasound by sonoluminescence: 5. Search for sonoluminescence *in vivo* in the human cheek," *Ultrasonics*, **28**, 181-184 (1990).
58. T. G. Leighton, S. D. Meers and P. R. White, "Propagation through nonlinear time-dependent bubble clouds, and the estimation of bubble populations from measured acoustic characteristics," *Proceedings of the Royal Society A,* **460**(2049), 2521-2550 (2004).
59. T. G. Leighton, "Characterization of measures of reference acoustic cavitation (COMORAC)", *J. Acoust. Soc. Am.,* **108**(5), Part 2, 2516 (2000).